Turun yliopisto
University of Turku

STRUCTURAL AND FUNCTIONAL STUDIES OF ANGUCYCLINE TAILORING ENZYMES

Pekka Patrikainen

TURUN YLIOPISTON JULKAISUJA – ANNALES UNIVERSITATIS TURKUENSIS
Sarja - ser. AI osa - tom. 517 | Astronomica - Chemica - Physica - Mathematica | Turku 2015

University of Turku

Faculty of Mathematics and Natural Sciences
Department of Biochemistry
Biochemistry
Doctoral Programme in Molecular Life Sciences

Supervised by

Docent Mikko Metsä-Ketelä, Ph.D.
Department of Biochemistry
University of Turku
Turku, Finland

Docent Jarmo Niemi, Ph.D.
Department of Biochemistry
University of Turku
Turku, Finland

Reviewed by

Docent Doreen Dobritzsch, Ph.D.
Department of Chemistry - BMC
Uppsala University
Uppsala, Sweden

Docent Lari Lehtiö, Ph.D.
Faculty of Biochemistry and Molecular
Medicine, Biocenter Oulu
University of Oulu
Oulu, Finland

Opponent

Professor Andreas Bechthold, Ph.D.
Institute for Pharmaceutical Sciences
Albert-Ludwigs-Universität Freiburg
Freiburg im Breisgau, Germany

ISBN 978-951-29-6155-9 (PRINT)
ISBN 978-951-29-6156-6 (PDF)
ISSN 0082-7002
Painosalama Oy - Turku, Finland 2015

CONTENTS

ABSTRACT

Polyketides are a diverse group of natural products produced in many bacteria, fungi and plants. These metabolites have diverse biological activities and several members of this group are in clinical use as antibiotics, anticancer agents, antifungals and immunosuppressants. The different polyketides are produced by polyketide synthases, which catalyze the condensation of extender units into various polyketide scaffolds. After the biosynthesis of the polyketide backbone, more versatility is created to the molecule by tailoring enzymes catalyzing for instance hydroxylations, methylations and glycosylations.

Flavoprotein monooxygenases (FPMO) and short-chain alcohol dehydrogenases/reductases (SDR) are two enzyme families that catalyze unusual tailoring reactions in the biosynthesis of natural products. In the experimental section, functions of homologous FPMO and SDR tailoring enzymes from five different angucycline pathways were studied *in vitro*. The results revealed how different angucyclinones are produced from a common intermediate and that FPMO JadH and SDR LanV are responsible for the divergence of jadomycins and landomycins, respectively, from other angucyclines.

Structural studies of these tailoring enzymes revealed differences between homologous enzymes and enabled the use of structure-based protein engineering. Mutagenesis experiments gave important information about the enzymes behind the evolution of distinct angucycline metabolites. These experiments revealed a correlation between the substrate inhibition and bi-functionality in JadH homologue PgaE. In the case of LanV, analysis of mutagenesis results revealed that the difference between the stereospecificities of LanV and its homologues CabV and UrdMred is unexpectedly related to the conformation of the substrate rather than to the structure of the enzyme.

Altogether, the results presented here have improved our knowledge about different steps of angucycline biosynthesis and the reaction mechanisms used by the tailoring enzymes behind these steps. This information can hopefully be used to modify these enzymes to produce novel metabolites, which have new biological targets or possess novel modes-of-action. The understanding of these unusual enzyme mechanisms is also interesting to enzymologists outside the field of natural product research.

Keywords: angucycline, biosynthesis, protein engineering

TIIVISTELMÄ

Polyketidit ovat luonnossa esiintyviä yhdisteitä, joita tuottavat useat eri bakteerit, sienet ja kasvit. Näillä yhdisteillä on monenlaisia biologisia aktiivisuuksia ja useita polyketidejä on kliinisessä käytössä antibiootteina, syöpälääkkeinä, sienilääkkeinä sekä immunosupressantteina. Näiden yhdisteiden hiilirunko muodostuu polyketidisyntaasien katalysoimien reaktioiden aikana. Muodostumisen jälkeen muokkausentsyymit lisäävät hiilirungon monimuotoisuutta katalysoimalla esimerkiksi hydroksylaatio-, metylaatio- ja glykosylaatioreaktioita.

Flavoproteiinimono-oksygenaasit (FPMO) ja lyhytketjuiset alkoholidehydrogenaasi/reduktaasi -entsyymit (SDR) ovat entsyymiperheitä, joiden jäseniä osallistuu muokkausreaktioiden katalysointiin luonnonyhdisteiden biosynteesissä. Kokeellisessa osassa selvitettiin viidestä eri angusykliinibiosynteesitiestä olevien homologisten FPMO- ja SDR-entsyymien funktioita. Nämä tulokset osoittivat kuinka samankaltaiset entsyymit saavat muutettua yhden yhteisen välituotteen eri angusykliineiksi. Samalla saatiin myös selville, että FPMO JadH ja SDR-entsyymi LanV katalysoivat reaktioita, joiden seurauksena jadomysiinit ja landomysiinit eroavat muista angusykliineistä.

Entsyymien rakennetutkimusten avulla saatiin selvitettyä miten homologisten entsyymien aktiiviset keskukset eroavat toisistaan. Mutageneesitutkimukset tuottivat mielenkiintoista informaatiota entsyymeistä, jotka ovat eri angusykliiniyhdisteiden evoluution takana. JadH:lle homologisen PgaE:n katalysoimista kahdesta peräkkäisestä hydroksylaatiosta huomattiin, että toisen hydroksylaation olemassaolo aiheuttaa substraatti-inhibition ensimmäisessä hydroksylaatioreaktiossa. LanV:n ja tämän homologin CabV:n välillä tehdyissä mutageneesitutkimuksissa taas huomattiin näiden entsyymien erilaisten stereospesifisyyksien johtuvan niiden käyttämien substraattien eroavista konformaatioista.

Tämän väitöskirjan tulokset selittävät eroavaisuuksia eri angusykliinien biosynteesien välillä sekä antavat uutta tietoa näiden entsyymien käyttämistä reaktiomekanismeista. Näitä uusia tietoja pystytään toivottavasti käyttämään näiden entsyymien muokkaukseen niin, että ne tuottavat uusia, biologisesti aktiivisia angusykliinejä. Lisäksi tässä väitöskirjassa selvitetyt entsyymien epätavalliset ominaisuudet kiinnostavat varmasti entsyymitutkijoita myös luonnonyhdistetutkimuksen ulkopuolella.

Asiasanat: angusykliinit, biosynteesi, proteiinimuokkaus

LIST OF ORIGINAL PUBLICATIONS

This thesis is based on the following publications, referred to as I–V in the text:

I Kallio, P., Patrikainen, P., Suomela, J.-P., Mäntsälä, P., Metsä-Ketelä, M., and Niemi, J. **(2011)** Flavoprotein Hydroxylase PgaE Catalyses Two Consecutive Oxygen-Dependent Tailoring Reactions in Angucycline Biosynthesis. *Biochemistry* **50**, 5535–5543.

II Patrikainen, P., Kallio, P., Fan, K., Klika, K. D., Shaaban, K. A., Mäntsälä, P., Rohr, J., Yang, K., Niemi, J., and Metsä-Ketelä. M. **(2012)** Tailoring Enzymes Involved in the Biosynthesis of Angucyclines Contain Latent Context Dependent Catalytic Activities. *Chemistry & Biology* **19**, 647–655.

III Kallio, P., Patrikainen, P., Belogurov, G. A., Mäntsälä, P., Yang, K., Niemi, J., and Metsä-Ketelä, M. **(2013)** Tracing the Evolution of Angucyclinone Monooxygenases: Structural Determinants for C-12b Hydroxylation and Substrate Inhibition in PgaE. *Biochemistry* **52**, 4507–4516.

IV Paananen, P.*, Patrikainen, P.*, Kallio, P., Mäntsälä, P., Niemi, J., Niiranen, L., and Metsä-Ketelä, M. **(2013)** Structural and Functional Analysis of Angucycline C-6 Ketoreductase LanV involved in the Landomycin Biosynthesis. *Biochemistry* **52**, 5304–5314. *Equal contribution.

V Patrikainen, P., Niiranen, L., Thapa, K., Paananen, P., Tähtinen, P., Mäntsälä, P., Niemi, J., and Metsä-Ketelä, M. **(2014)** Structure-Based Engineering of Angucyclinone 6-Ketoreductases. *Chemistry & Biology* **21**, 1381–1391.

ABBREVIATIONS

ACP	acyl carrier protein
AT	acyl transferase
BIQ	benzoisochromanequinones
CoA	coenzyme A
CPA	chromopyrrolic acid
DFT	density functional theory
DH	dehydratase
DNPA	4-dihydro-9-hydroxy-1-methyl-10-oxo-3-*H*-naphtho[2,3-*c*]pyran-3-acetic acid
dTDP	thymidine diphosphate
EAC	escape from adaptive conflict
ECD	electronic circular dichroism
ER	enoyl reductase
ESI	electrospray ionization
ESI-HRMS	electrospray ionization-high-resolution mass spectrometry
FAD	flavin adenine dinucleotide
FMN	flavin mononucleotide
FPMO	flavoprotein monooxygenases
GALE	UDP-galactose-4-epimerase
GDP	guanosine diphosphate
GFS	GDP-fucose synthase
GME	GDP-mannose-3',5'-epimerase
HPLC	high-performance liquid chromatography
KR	ketoreductase
KS	ketosynthase

LC-MS	liquid chromatography-mass spectrometry
MCoA	malonyl-CoA
MIC	minimum inhibitory concentration
minPKS	minimal polyketide synthase
mMCoA	methylmalonyl-CoA
NAD^+	nicotinamide adenine dinucleotide
NADH	reduced form of nicotinamide adenine dinucleotide
$NADP^+$	nicotinamide adenine dinucleotide phosphate
NADPH	reduced form of nicotinamide adenine dinucleotide phosphate
NDP	nucleoside diphosphate
ORF	open reading frame
PCR	polymerase chain reaction
PDB	Protein Data Bank
PKS	polyketide synthase
PHBH	*para*-hydroxybenzoate hydroxylase
PHHY	phenol hydroxylase
rmsd	root-mean-square deviation
RP-HPLC	reverse-phase high-performance liquid chromatography
SDR	short-chain alcohol dehydrogenase/reductase
SDS-PAGE	sodium dodecyl sulfate-polyacrylamide gel electrophoresis
SPE	solid phase extraction
UDP	uridine diphosphate
UV-vis	ultraviolet-visible

ABBREVIATIONS OF THE AMINO ACID RESIDUES

A	Ala	Alanine
C	Cys	Cysteine
D	Asp	Aspartic acid
E	Glu	Glutamic acid
F	Phe	Phenylalanine
G	Gly	Glycine
H	His	Histidine
I	Ile	Isoleucine
K	Lys	Lysine
L	Leu	Leucine
M	Met	Methionine
N	Asp	Asparagine
P	Pro	Proline
Q	Gln	Glutamine
R	Arg	Arginine
S	Ser	Serine
T	Thr	Threonine
V	Val	Valine
W	Trp	Tryptophan
Y	Tyr	Tyrosine
X	Any amino acid	

1. INTRODUCTION

1.1 Biosynthesis of polyketide natural products

Natural products are the largest source of new scaffolds for drug molecules in the world, since 39% of all approved drugs between the years 1981 and 2010 were natural products or their synthetic derivatives. In the case of antibacterial drugs, this percentage was even higher, rising to 66% (Newman and Cragg, 2012). This highlights the importance of natural products in drug development, especially in the case of antibacterials, but also medicines in general. Despite the focus of drug industry on large libraries of synthetic molecules, natural products have remained a main source of new chemical entities in drugs, as in 2010, 50% of all approved drugs were natural products or their synthetic derivatives (Newman and Cragg, 2012, Wright, 2014).

Polyketides are one of the largest and most diverse groups of natural products, and they are produced by different species of bacteria, fungi and plants (Hertweck, 2009). These secondary metabolites are well known for their biological activities, and they are in clinical use as antibiotics (tetracycline, erythromycin A, rifamycin S), anticancer agents (doxorubicin, epothilones), antifungals (amphotericin B, nystatin) and immunosuppressants (rapamycin, ascomycin) (Figure 1). Besides these examples of polyketides used as medicines, several other polyketide metabolites outside the clinical use, have been shown to exhibit various biological activities with different modes-of-action (Lombo et al., 2006, Korynevska, et al., 2007, Kharel et al., 2010, Osmanova et al., 2010)

The polyketide metabolites are produced by different polyketide synthases (PKS) that catalyze consecutive Claisen condensations of different small organic acids into long polyketide chains (Khosla et al., 2014, Hertweck, et al., 2007, Stewart et al., 2013). Type I PKS are large modular multidomain enzymes in which each module catalyzes one condensation reaction followed by the transfer of the growing polyketide chain to the next module. These modules are comprised of ketosynthase (KS), acyl transferase (AT) and acyl carrier protein (ACP) domains together with optional ketoreductase (KR), dehydratase (DH) and enoyl reductase (ER) domains. The KR, DH and ER domains are present in different combinations and are responsible for the processing of the β-keto groups (Figure 2A) (Hertweck, 2009, Khosla et al., 2014).

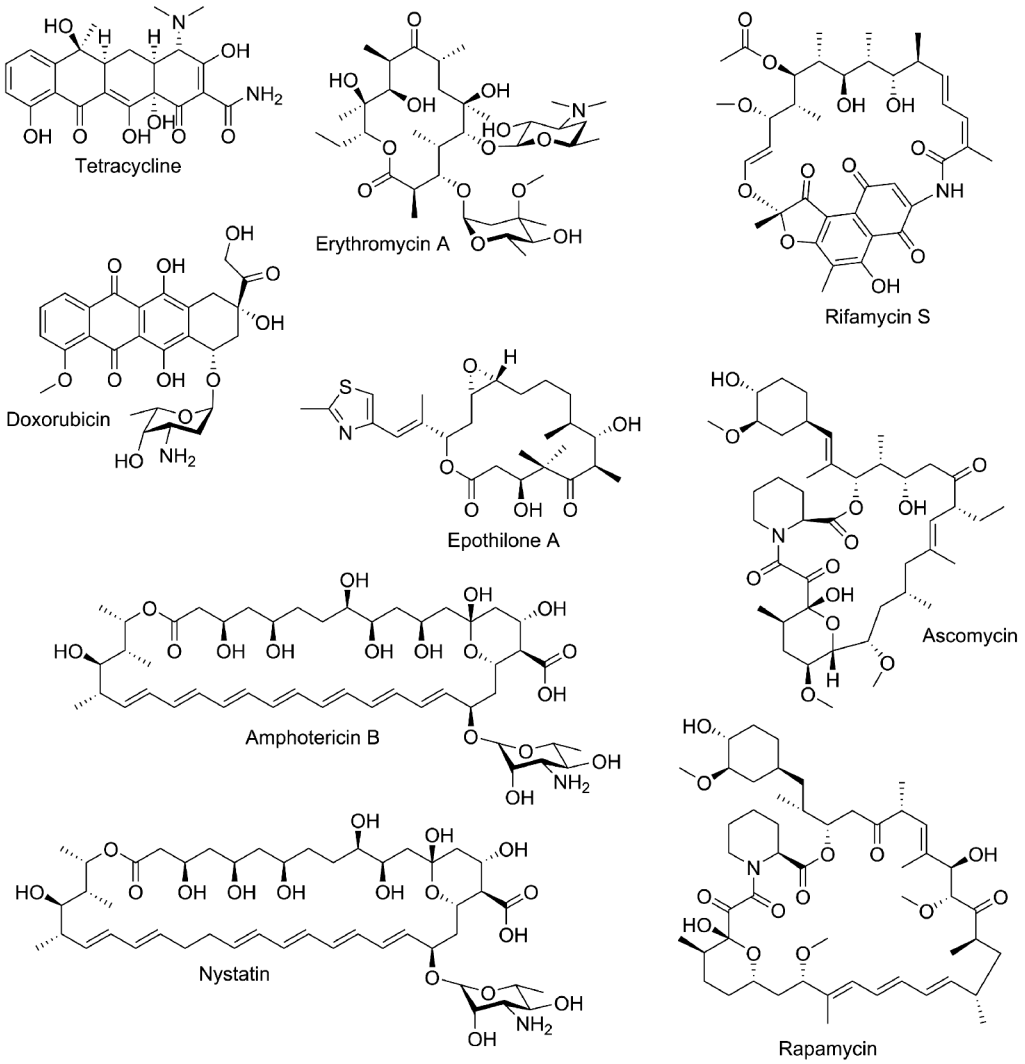

Figure 1: Chemical structures of polyketide natural products tetracycline, erythromycin A, rifamycin S, doxorubicin, epothilone A, ascomycin, amphotericin B, nystatin and rapamycin.

In contrast to type I PKS, type II PKS are multienzyme complexes in which distinct enzymes are translated from individual genes. The polyketide scaffold in type II PKS is produced by a so-called minimal PKS complex (minPKS), which consists of two ketosynthases, KS_{α} and KS_{β} (KS_{β} is also known as a chain length factor), and an ACP. After the formation of the polyketide chain, cyclases, aromatases and KR enzymes catalyze reactions that define the final folding pattern of these metabolites (Figure 2B) (Hertweck, et al., 2007, Hertweck, 2009). For example in the case of decaketides produced by type II PKS, specific cyclases that close the fourth ring in an angular position are responsible for the formation of an angucycline-type scaffold instead of the linear four-ring structure present in tetracyclines and anthracyclines (Metsä-Ketelä et al., 2003, Hertweck et al., 2007).

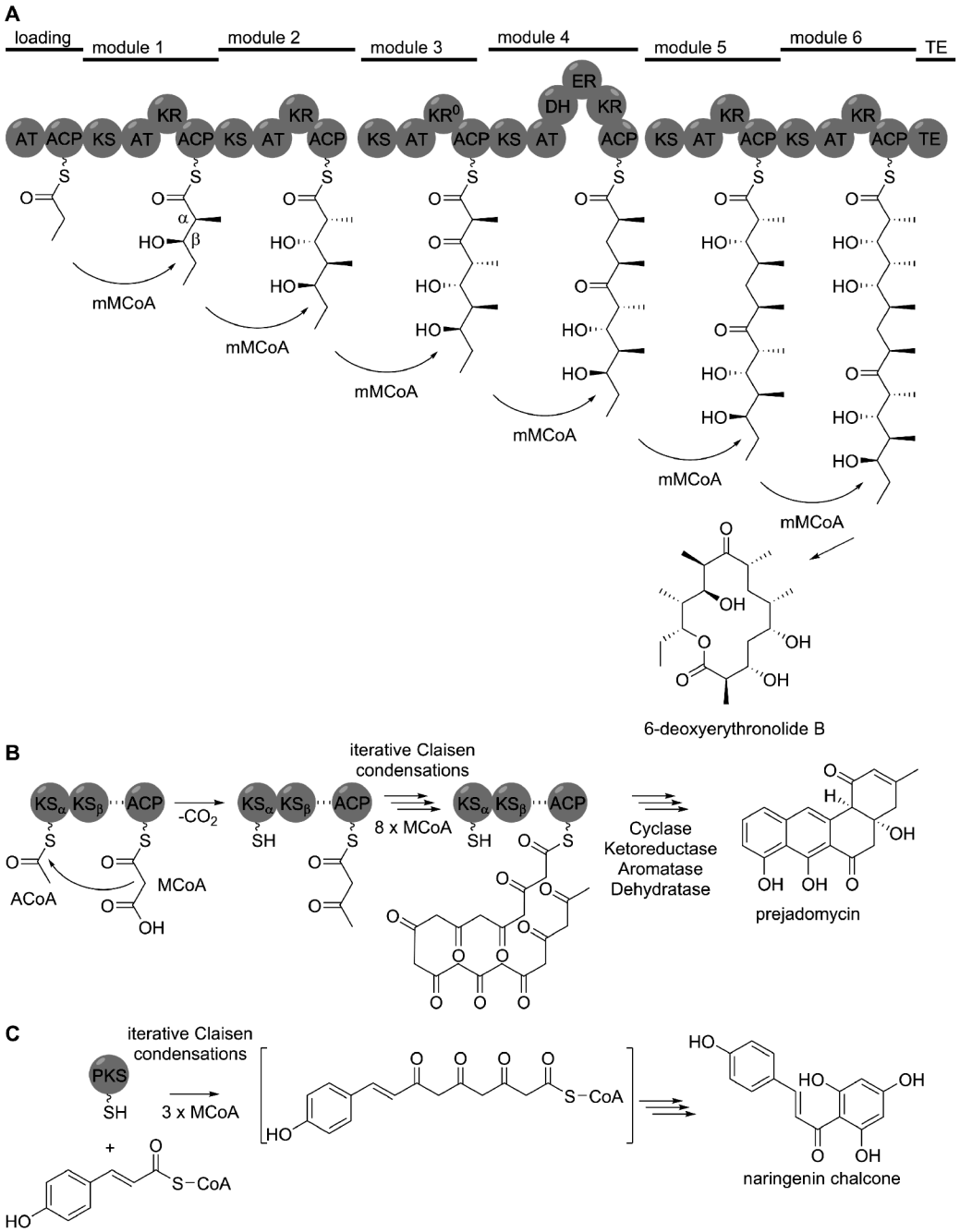

Figure 2: Reactions catalyzed by (A) type I, (B) type II and (C) type III polyketide synthases as exemplified by deoxyerythronolide-B-synthase, angucycline type-synthase and chalcone synthase, respectively. KR^0 in module 3 of deoxyerythronolide-B-synthase is ketoreductase-inactive but is involved in the epimerization of α-methyl group (Garg et al., 2014). mMCoA = methylmalonyl-CoA, MCoA = malonyl-CoA. Figure adapted from Khosla et al., 2007, Hertweck, 2009 and Kang et al., 2014.

The simplest PKS are represented by type III PKS, which are homodimers that catalyze all the reactions necessary for the formation of the polyketide backbone in one catalytic center (Figure 2C). In contrast to all other PKS, they have no ACP but use coenzyme A (CoA) tethered substrates in thioester exchange reactions (Stewart et al., 2013, Hertweck, 2009).

In all polyketide types, the backbone chain produced by the PKS is further modified by tailoring enzymes. These enzymes, which catalyze reactions like hydroxylations, ketoreductions, methylations and glycosylations, create more versatility in the already large pool of natural product backbones and are one of the major factors behind the vast structural diversity of polyketide metabolites (Rix et al., 2002, Hertweck et al., 2007).

Because of the constant increase in the number of multi-antibiotic-resistance pathogens and drug-resistant tumor cells, we have a growing need for new antibiotics (Wright, 2014). One possible way to create new antibiotics is pathway engineering. The general idea of pathway engineering is to modify the properties of a known pathway or combine features from different pathways to produce novel metabolites. However, in order to modify the biosynthetic pathways of polyketides, we have to understand how the different steps in their biosynthesis are catalyzed (Walsh, 2002). Another possibility to generate novel natural products is protein engineering, where biosynthetic enzymes are modified to catalyze novel reactions. A thorough understanding of the enzyme mechanism and structure is vital for the success of this kind of approach (Zabala et al., 2012a).

Both flavoprotein monooxygenases (FPMO) and short-chain alcohol dehydrogenases/reductases (SDR) are found as tailoring enzymes in several different natural product pathways. Members of these protein families catalyze a wide range of different tailoring reactions to various different substrates. Since these enzymes are crucial for the diversity of natural products, they are among the most potent tools for the generation of modified natural product pathways, which are not normally found from nature (Thibodeaux et al., 2008, Wang et al., 2012a).

1.2 Flavoprotein monooxygenases in the biosynthesis of natural products

One large group of tailoring enzymes involved in the biosynthesis of natural products are the flavoprotein monooxygenases, which use a flavin cofactor to activate molecular oxygen and incorporate one oxygen atom into the target substrate while the second oxygen is reduced to water. These enzymes are involved in several types of oxygenation reactions in the biosynthesis of natural products, including aromatic polyketides. Tailoring reactions catalyzed by the FPMOs include, for instance, hydroxylations, epoxidations, and Bayer-Villiger reactions (Crozier-Reabe and Moran, 2012).

The catalytic cycle of oxygen incorporation by FPMOs begins with the reduction of the flavin cofactor, which is required for the activation of molecular oxygen. Most of the FPMOs are so-called external FPMOs, which use the reduced form of nicotinamide

adenine dinucleotide (NADH) or nicotinamide adenine dinucleotide phosphate (NADPH) to reduce flavin. Internal FPMOs are an exceptional subclass of FPMOs as they use their own substrate in the reduction of the flavin cofactor (van Berkel et al., 2006).

Based on their biochemical properties, sequences and structures, external FPMOs are divided into several subclasses. Members of the Class A and B are encoded by one gene and contain a tightly bound flavin adenine dinucleotide (FAD), which is reduced by NAD(P)H (Class A) or NADPH (Class B). FPMOs from Class C–E are mostly two-component systems, which utilize an NAD(P)H of a reductase component to reduce flavin mononucleotide (FMN) (Class C) or FAD (Class D-F) (van Berkel et al., 2006, Crozier-Reabe and Moran, 2012). Members of the Class F are exceptional among FPMOs since they catalyze halogenations instead of oxygen additions (Huijbers et al., 2014).

All of the Class A FPMOs have two common domains: an FAD binding domain and an N-terminal domain that forms the other side of the substrate binding pocket. The active site of the enzyme resides between these two domains (Crozier-Reabe and Moran, 2012). Enzymes of this class have one glutathione reductase type Rossmann fold, which is used to bind FAD, but no binding site for NAD(P)H has been recognized (van Berkel et al., 2006, Huijbers et al., 2014). Some FPMOs, like phenol hydroxylase (PHHY), PgaE and RebC, also have a third, C-terminal domain, but the function of this domain is not known (Crozier-Reabe and Moran, 2012). Discussion in this thesis focuses on the Class A FPMOs because angucycline monooxygenases PgaE and CabE discussed in the experimental section are also members of this subclass.

1.2.1 Reaction mechanism of the Class A flavoprotein monooxygenases

Although oxygen is found in a plethora of metabolites in nature, the insertion of oxygen into an organic substrate is extremely difficult. To catalyze this spin-forbidden reaction between oxygen and carbon, the enzyme has to activate molecular oxygen (van Berkel et al., 2006). The reaction mechanism used by the Class A FPMOs to activate oxygen and catalyze its insertion into organic compounds has been extensively studied, mainly with the enzymes *para*-hydroxybenzoate hydroxylase (PHBH) (Entsch et al., 1976, Wierenga et al., 1979, Entsch and van Berkel, 1995) and PHHY (Enroth et al., 1998, Enroth, 2003). The reductive half reaction starts from the resting state of the enzyme in which the isoalloxazine ring of the FAD is in so-called OPEN/IN conformation, enabling the entry of the substrate into the active site (Wang et al., 2002, Crozier-Reabe and Moran, 2012). The binding of the substrate has been shown to increase the ability of the enzyme to reduce FAD with NADPH by 140,000-fold (Husain and Massey, 1979). The substrate binding followed by the binding of NAD(P)H causes a conformational change in the FAD from IN to OUT, which presents the *re*-face of the isoalloxazine to the NAD(P)H, enabling the reduction of the cofactor FAD (Figure 3, step 1). After the reduction of FAD, $NAD(P)^+$ is slowly released from the active site, and the positive electrostatic environment of the active site attracts the negatively charged isoalloxazine ring back to the IN conformation (Crozier-Reabe and Moran, 2012).

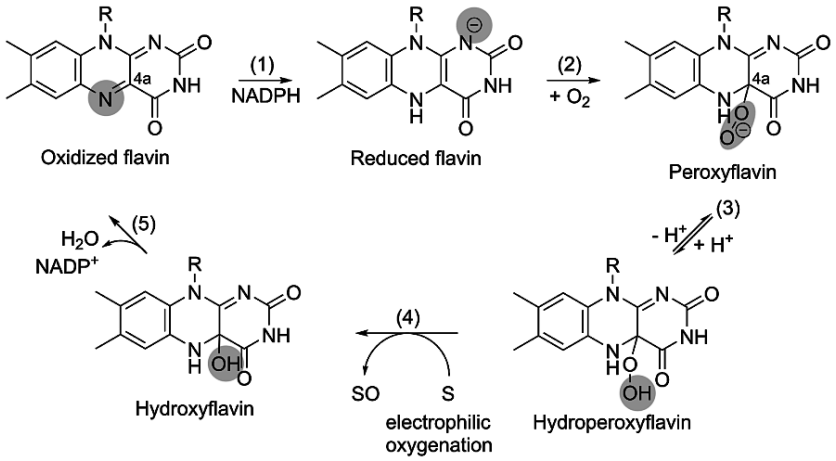

Figure 3: The redox cycle of FAD during the catalysis in Class A FPMOs. Steps 1–5 are explained in the main text. The substrate S consumed in step 4 is bound to the active site of the enzyme prior to step 1 and the oxygenated product SO is released during step 4. Steps 4 and 5 occur simultaneously. The shading used in this and following figures indicates the part of the molecule, which has changed during the previous reaction step. R in FAD consists of a ribityl phosphate moiety connected to adenosine monophosphate; the ribityl moiety is connected to isoalloxazine ring.

The oxidative half reaction of the Class A FPMOs starts from a situation where the substrate is in the active site of the enzyme, the reduced FAD is back in the IN conformation and dioxygen lies next to the C-4a of the isoalloxazine ring in the solvent-free environment. The following electron transfer from the reduced flavin to the molecular oxygen creates two radical species: a superoxide anion and a flavin semiquinone. The second electron transfer from the flavin radical to the superoxide takes place through spin inversion followed by the recombination of the two radicals (Figure 3, step 2). The formed C-4a-peroxyflavin is stabilized by the enzyme and protonated into a hydroperoxy form (Figure 3, step 3) before it is attacked by the substrate in an electrophilic oxygenation, which results in an incorporation of one oxygen atom into the substrate (Figure 3, step 4). At the same time, the other oxygen atom is reduced to a water molecule (Figure 3, step 5) (Crozier-Reabe and Moran, 2012).

1.2.2 Hydroxylation reactions in the biosynthesis of natural products

Several different FPMOs are involved in the hydroxylation reactions of natural products. These reactions typically follow the canonical mechanism for the FPMOs using FAD to hydroxylate their aromatic substrates. Some examples of classical hydroxylases in the biosynthesis of natural products are the aklavinone-11-hydroxylase RdmE (Niemi et al., 1999), VioC and VioD from violacein pathway (Balibar and Walsh, 2006), and SibG involved in the biosynthesis of sibiromycin (Giessen et al., 2011). The hydroxylases reviewed in the following sections show some characteristics that extend beyond this basic hydroxylation paradigm (Huijbers et al., 2014).

1.2.2.1 OxyS catalyzes hydroxylations in oxytetracycline biosynthesis

Tetracyclines are a group of aromatic type II polyketides with a four-ring carbon scaffold and a broad-spectrum of antibiotic activities. Several different tetracycline derivatives are in clinical use as antibiotics, but the emergence of tetracycline resistant bacterial strains has reduced their efficacy in clinical applications. The biosynthesis of tetracycline in *Streptomyces aureofaciens* (Darken et al., 1960) and oxytetracycline in *S. rimosus* (Finlay et al., 1950) are known to have a common late intermediate, anhydrotetracycline, (Zhang et al., 2008, Pickens and Tang, 2010). One of the main differences between the biosynthesis of these two compounds is the C-5 hydroxyl group, which is present in oxytetracycline but missing from tetracycline (Figure 4).

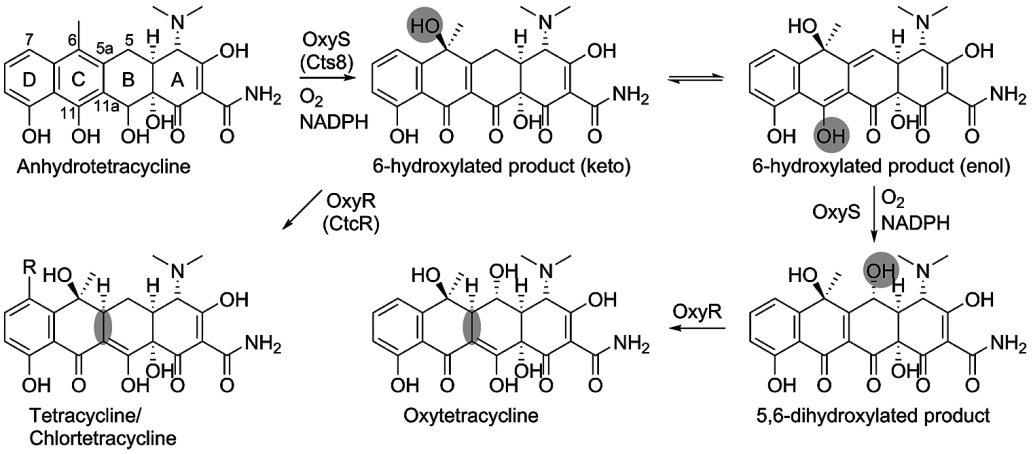

Figure 4: The biosynthesis of tetracycline and oxytetracycline from anhydrotetracycline by the action of flavoprotein monooxygenase OxyS and F_{420}-dependent reductase OxyR. OxyS and OxyR homologues Cts8 and CtcR, respectively, consume 7-chlorinated substrates in chlortetracycline biosynthesis. R is H in tetracycline and Cl in chlortetracycline. Figure adapted from Wang et al., 2013.

A flavoprotein monooxygenase OxyS from *S. rimosus* and its homologue Cts8 from *S. aureofaciens* have been shown to catalyze the 6-hydroxylation of anhydrotetracycline (Peric-Concha et al., 2005, Wang et al., 2012b, Vancurova et al., 1988). The recent *in vitro* studies by the group of Prof. Tang have shown that OxyS is also responsible for the 5-hydroxylation step in the biosynthesis of oxytetracycline. The incubation of anhydrotetracycline with OxyS and OxyR, an F_{420}-dependent 5a,11a-reductase, in the presence of reduced coenzyme F_{420} and NADPH, yielded both oxytetracycline and tetracycline (Figure 4) (Wang et al., 2013).

The 6-hydroxylation of anhydrotetracycline is expected to take place through the canonical reaction mechanism of FPMOs by using O_2 and NADPH as co-substrates and FAD as a co-factor. After this hydroxylation, the product is released from the active site and bound again for the 5-hydroxylation to take place. This release is

one of the key factors behind the differences between oxytetracycline, tetracycline and chlorotetracycline. The absence of a C-5 hydroxyl group in tetracycline and chlortetracycline can be explained by the differences in the substrate affinities of OxyR and its homologue CtcR from *S. aureofaciens* toward the 6-hydroxylated anhydrotetracycline (Wang et al., 2013, Ryan, 1999). *In vitro* results show that compared to OxyR, CtcR has a higher affinity toward this product than OxyS, a difference which could steer the biosynthesis from oxytetracycline to chlorotetracycline. At the same time, the lower affinity of OxyR toward the 6-hydroxylated anhydrotetracycline enables the production of both tetracycline and oxytetracycline by OxyS (Figure 4) (Wang et al., 2013).

The product of the 6-hydroxylation has an equilibrium between keto and enol forms around carbons C-11, C-11a, C-5a and C-5, and the enol form is the expected substrate for the 5-hydroxylation of OxyS. The extraction of the proton from the C-11 hydroxyl of the enol form by a catalytic base can cause the formation of C-5 carbanion which can then attack the hydroperoxyflavin in the active site of OxyS. The opposite stereochemistries of C-5 and C-6 hydroxyl groups in oxytetracycline can be explained by changes in the conformation of the active site cavity that tilt the substrates, anhydrotetracycline and the 6-hydroxy-anhydrotetracycline, to facilitate the attack of the FAD from opposite sides (Wang et al., 2013).

The 2.6 Å resolution crystal structure of OxyS in complex with oxidized FAD (Protein Data Bank (PDB) code 4K2X) revealed an overall structure that is very similar to other FPMOs like aklavinone 11-hydroxylase RdmE and prejadomycin hydroxylases PgaE and CabE. The modeling of anhydrotetracycline to the structure of OxyS using RdmE co-crystallized with aklavinone as a template revealed two amino acids, His-47 and Phe-215, that appear to have close contacts with the ligand. These residues are facing the ligand from the opposite sides positioning the ligand between them. The mutation of these to alanine and isoleucine, respectively, led to changes in the ratio of the produced tetracycline and oxytetracycline, indicating that these residues affect the correct alignment of the substrates for C-5 and C-6 hydroxylation reactions (Wang et al. 2013).

1.2.2.2 AzaH affects to the pyran-ring formation in azaphilones

Azaphilones are a group of fungal metabolites that are characterized by a highly oxidized bicyclic pyranone-quinone core (Figure 5A) (Osmanova et al., 2010). Azanigerones A–F are azaphilones produced by the silent *aza* gene cluster from *Aspergillus niger* ATCC1015, where the polyketide scaffold is generated by both highly reducing PKS (*azaB*) and non-reducing PKS (*azaA*) (Zabala et al., 2012b).

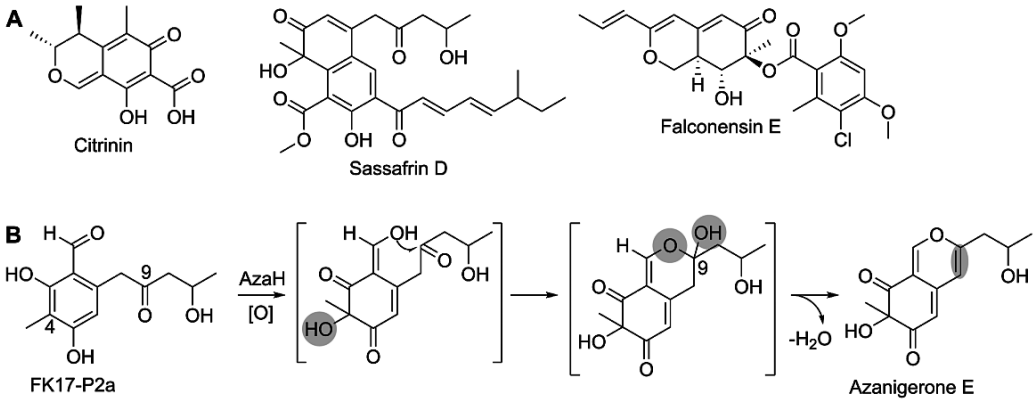

Figure 5: (A) Examples of azaphilone metabolites isolated from different fungi. Citrinin is an inhibitor of the cholesterol synthesis isolated i.a. from *Monascus* sp., sassafrin D is a broad-spectrum antibiotic from *Creosphaeria sassafras* and falconensin E has anti-inflammatory activity and is isolated from *Emericella falconensis* (Osmanova et al., 2010). (B) The hydroxylation reaction catalyzed by AzaH and the consequent pyran-ring formation in the biosynthesis of azanigerones. FK17-P2a is the proposed product of the putative ketoreductase AzaE. Panel B adapted from Zabala et al., 2012b.

The reaction catalyzed by AzaH, a flavoprotein monooxygenase from the *aza* gene cluster, was confirmed by *in vitro* experiments using an intermediate of the azanigerone biosynthesis, FK17-P2a, as a substrate. FK17-P2a is an early culture product that is detectable only in the early days of the activated *A. niger* T1 culture and is suggested to be the reaction product of the putative ketoreductase AzaE. The *in vitro* analysis showed that AzaH alone is sufficient to convert FK17-P2a to a bicyclic product, azanigerone E, which has gone through the hydroxylation of C-4, pyran-ring formation and the loss of hydroxyl group from C-9 (Figure 5B). This analysis confirmed that the AzaH catalyzed hydroxylation is required for the consequent pyran-ring formation in the azanigerone biosynthesis (Zabala et al., 2012b).

1.2.2.3 TetX confers resistance to tetracycline antibiotics

One of the many biological functions of the FPMOs is the degradation of xenobiotics (Entsch and van Berkel, 1995, Ballou et al., 2005, Alfieri et al., 2008). The first FMPO that has been shown to catalyze the inactivation of antibiotics is the product of gene *tetX* (Yang et al., 2004). The gene *tetX*, as well as its orthologues *tetX1* (66% amino acid sequence identity) and *tetX2* (99% identity), have been found from the transposons of different *Bacteroides* species (Speer and Salyers, 1988, Park and Levy, 1988, Whittle et al., 2001). The transformation of *Escherichia coli* W3110 with a plasmid containing the *tetX* or *tetX2* gene conferred resistance to tetracycline, but the N-terminally truncated version *tetX1* was unable to confer resistance (Yang et al., 2004).

TetX2 is an FPMO that has been shown to catalyze the inactivation of tetracycline and its derivatives oxytetracycline, chlortetracycline, demeclocycline, doxycycline,

and minocycline while TetX has been shown to inactivate tigecycline (Figures 4 and 6A). The analysis of the TetX2 and TetX inactivation products of oxytetracycline and tigecycline revealed 11a-hydroxylated compounds P1 and 11a-hydroxytigecycline, respectively (Yang et al., 2004, Moore et al., 2005). The P1 product was found to be very unstable under the reaction conditions (pH 8.5), and degradation was prevented only at very acidic conditions (pH 1). A time-course high-performance liquid chromatography (HPLC) analysis of the TetX2 reaction with oxytetracycline showed consumption of the substrate, production of the P1 product and conversion of P1 to P2 product. The molecular mass of P2 corresponds to a loss of water molecule from P1, and the compound was found to be unstable (Yang et al., 2004). The 11a-hydroxytigecycline, on the other hand, was found to be stable under the reaction conditions (Moore et al., 2005).

The activities of tigecycline and 11a-hydroxytigecycline were tested against *E. coli* W3110 strain. The minimum inhibitory concentration (MIC) value of 11a-hydroxytigecycline was shown to be 64 μg/ml whereas the MIC for tigecycline was only 0.5 μg/ml. However, the MIC value of the tigecycline against *E. coli* W3110 strain harbouring the *tetX* gene was only 2 μg/ml, showing that, although TetX can use tigecycline as a substrate, this third generation tetracycline can still be active against *tetX*-positive strains (Moore et al., 2005).

The structural analysis of TetX in complex with different tetracycline derivatives has revealed the basis of the wide substrate specificity exhibited by this tetracycline inactivating enzyme. The structures of TetX with bound FAD in the IN conformation and tetracyclines 7-iodtetracycline (PDB code 2Y6Q), 7-chlortetracycline (2Y6R), minocycline (4A99) and tigecycline (4A6N) show that all tetracyclines are bound by TetX in a similar manner; FAD stabilizes the substrate binding, and the hydrophobic (substituents at C-5–C-9) and hydrophilic (C-1–C-4 and C-10–C-12) parts of the tetracyclines are in contact with the hydrophobic and hydrophilic regions of the active site, respectively (Figure 6A and 6B). The most conserved interactions in the different TetX structures are the hydrogen bonds between O-4 and N-5 atoms of the FAD and C-12 and C-12a hydroxyl groups of the different tetracycline ligands, the hydrogen bond from Arg-213 to O-1 atom of the FAD and the hydrogen bonds between the Gln-192 and the substituents in the A-ring of tetracyclines (Figure 6C). In all of the structures, the distance between the C-4a of FAD and the C-11a hydroxylation site of tetracyclines is appropriate for a hydroxylation reaction to take place (5.9–6.0 Å). Also, all the structures show that the D-ring and substituents in it are exposed to bulk solvent (Volkers et al., 2011, Volkers, et al., 2013).

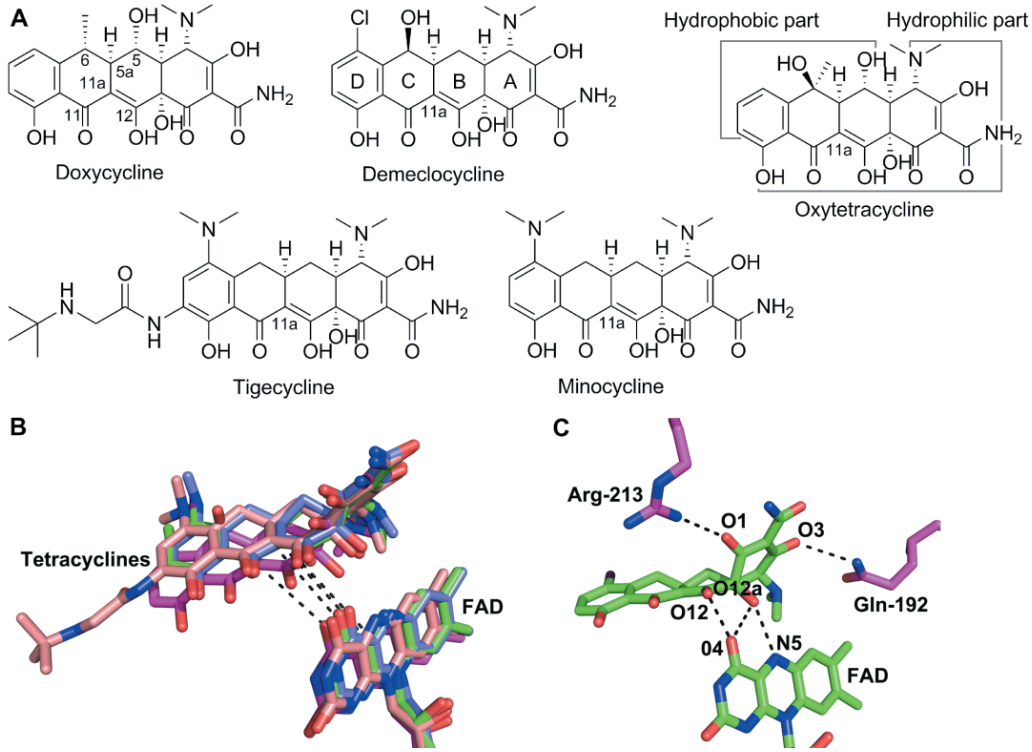

Figure 6: (A) Structures of the different tetracyclines in which 11a-hydroxylation is catalyzed by TetX or TetX2. The hydrophobic and hydrophilic parts of tetracyclines are highlighted with grey line on oxytetracycline. (B) An overlay of TetX bound 7-iodtetracycline (green) (PDB code 2Y6Q), 7-chlortetracycline (magenta) (2Y6R), minocycline (light blue) (4A99) and tigecycline (salmon) (4A6N). (C) The FAD and 7-iodtetracycline in the active site of TetX. Dashed black lines represent (B) the distance between C-4a of FAD and C-11a of different tetracyclines or (C) the most conserved interactions between TetX and different tetracyclines.

All the most important interactions between the tetracycline substrates and TetX are on the regions that are conserved in all the different tetracycline antibiotics. The modifications in the D-ring, like the 9-*tert*-butylglycylamido group at the C-9 of tigecycline, are exposed to solvent and hence will not affect the ability of TetX to bind these tetracyclines. Since oxygens at positions C-11 and C-12 of tetracyclines are involved in the Mg^{2+} ion coordination, which is important for the biological activity, only modifications in the A-ring could be used to generate fourth generation tetracyclines, which would overcome all currently known tetracycline resistance mechanisms (Brodersen et al., 2000, Volkers et al., 2011, Volkers, et al., 2013).

1.2.3 RebC and StaC in the branching point of indolocarbazoles

Rebeccamycin, a DNA-topoisomerase I inhibitor, and staurosporine, a protein kinase inhibitor, are members of an indolocarbazole class of natural products (Bailly et al., 1997, Rüegg and Burgess, 1989) (Figure 7A). The central indolo[2,3-a]pyrrole[4,3-c]

carbazole ring system is derived from two tryptophan residues by the enzymes RebODPC from *Lechevalieria aerocolonigenes* and StaODPC from *Streptomyces* sp. TP-A0274. RebO and StaO are amino acid oxidases, RebD and StaD chromopyrrolic acid synthases, RebP and StaP cytochrome P450 enzymes and RebC and StaC FPMOs (Pearce et al., 1988, Meksuriyen and Cordell, 1988, Sanchez et al., 2005, Howard-Jones and Walsh, 2006).

RebC and StaC both have all three structural motifs typical to flavoprotein hydroxylases (see chapter 1.2) and are involved in the formation of the differently oxygenated aglycones of indolocarbazoles rebeccamycin and staurosporine, respectively. RebC and StaC work together with RepP or StaP to convert chromopyrrolic acid (CPA) into arcyriaflavin A and K252c, respectively (Figure 7B). *In vitro* experiments have shown that StaP with NADH, spinach ferredoxin and *E. coli* flavodoxin $NADP^+$-reductase converts CPA into three products: K252c, 7-hydroxy-K252c and arcyriaflavin A in a 1:7:1 ratio. The addition of RebC or StaC into this reaction mixture yielded only arcyriaflavin A or K252c, respectively. These results show that, although the K252c and arcyriaflavin A can be produced by StaP alone, StaC and RebC can clearly mediate the efficient catalysis of the net 4-electron and 8-electron oxidations, which are required for the formation of K252c and arcyriaflavin A, respectively (Howard-Jones and Walsh, 2006).

Protein X-ray crystallography experiments with RebC and RebC-10x (RebC mutant where 10 amino acids have been changed to corresponding StaC residues and which catalyzes the formation a K252c) have given insights into the catalytic mechanisms of RebC and StaC (Ryan et al., 2007, Ryan et al., 2008, Goldman et al., 2012). Under aerobic conditions in room temperature, CPA has been shown to partially degrade into K252c, 7-hydroxy-K252c and arcyriaflavin A and some minor products like 7-carboxy-K252c (Figure 7B). This same degradation is also seen during the long soaking of RebC and RebC-10x crystals with CPA, as both of these enzymes were able to selectively bind the 7-carboxy-K252c from the mixture of the degradation products. The modeling of CPA degradation products into the electron densities found in the active sites suggested that RebC can most likely bind both keto and enol forms of 7-carboxy-K252c whereas the keto form is best fitted to the electron density in the active site of RebC-10x (Ryan et al., 2007, Goldman et al., 2012). Crystal structures of RebC have revealed that the isoalloxazine moiety of FAD goes through similar movements as in the well-studied PHBH; in the native structure of RebC, the isoalloxazine ring is in the OUT position and the binding of the substrate induces a conformational change of FAD into IN position (Figure 8A) (Ryan et al., 2007). Also, the reduction of FAD causes the isoalloxazine moiety to move from OUT to IN position (Ryan et al., 2008). However, the binding of the K252c, which lacks the carboxy at C-7, does not induce the conformational OUT to IN change in RebC, suggesting that this is not a true substrate for RebC (Ryan et al., 2007).

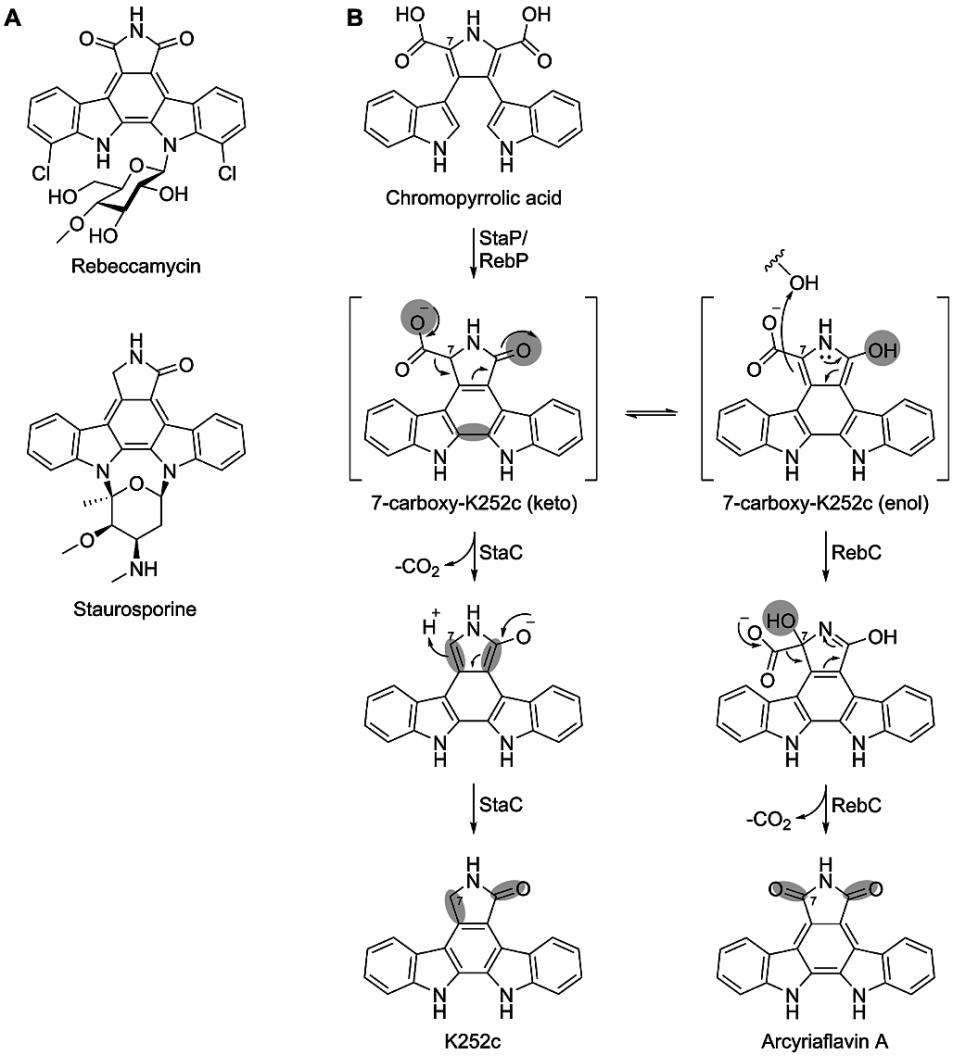

Figure 7: (A) Structures of indolocarbazoles rebeccamycin and staurosporine. (B) The reactions catalyzed by RebC and StaC in the biosynthesis of rebeccamycin and staurosporine, respectively. Panel B adapted from Goldman et al., 2012.

The structures of RebC and RebC-10x with their expected substrates showed some interesting differences in the interactions between FAD, the substrate and the enzymes (Ryan et al., 2007, Goldman et al., 2012). In RebC, arginines Arg-239 and Arg-230 are within hydrogen bonding distance from one of the oxygens in the carboxyl moiety of the ligand. At the same time, the C-4a carbon of FAD is 5.1 Å away from the C-7 of the ligand, which resembles the distance between C-4a and the site of hydroxylation in PHHY and its substrate (5.3 Å) (Enroth 2003, Ryan et al., 2007). In RebC-10x, the Arg-239 has been replaced with the corresponding StaC amino acid asparagine, and because of the changes G48S and F216V the Arg-230 adopts a "lower" position (Figure 8B).

These changes appear to prefer the binding of the keto tautomer of 7-carboxy-K252c instead of the enol form (Goldman et al., 2012).

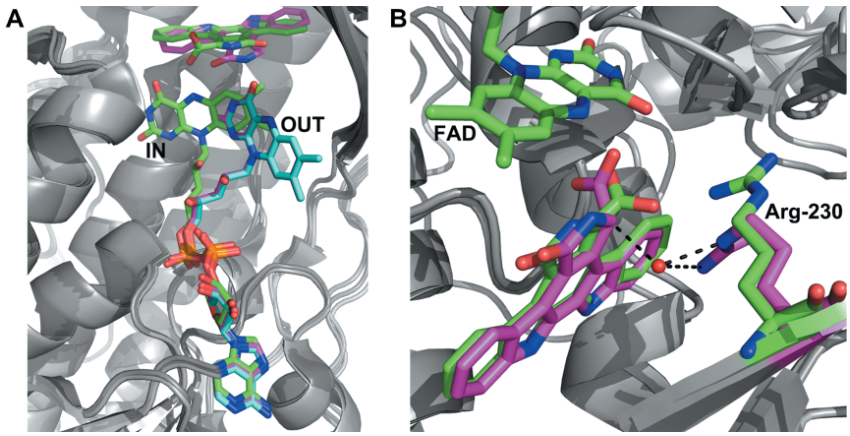

Figure 8: (A) Close-up view of the active site of RebC with bound FAD and 7-carboxy-K252c (green) (PDB code 2R0G), K252c (violet) (2R0P) and no ligand (cyan) (2R0C). The FAD can be seen in both IN (green) and OUT (violet and cyan) conformations. (B) Close-up view of the active sites of RebC with bound FAD and keto form of 7-carboxy-K252c (green) (2R0G) and RebC-10x with bound enol form of 7-carboxy-K252c (4EIQ). Arg-230 residues in RebC and RebC-10x are shown in green and violet, respectively, and the ordered water molecule in the active site of RebC-10x as a red sphere.The interactions between this water molecule, C-7 position of 7-carboxy-K252c and the nitrogens of Arg-230 are shown as black dashed lines.

Based on the functional and structural information gained from the different experiments conducted with RebC, StaC and their mutant versions, reaction mechanisms have been suggested to RebC and StaC by the Drennan group (Goldman et al., 2012). The observation that RebC and StaC have the same substrate but it binds in different tautomeric forms suggests that differences in these tautomers could mediate the formation of two different products. The sp^3 hybridized C-7 in the keto tautomer could accept electrons from the spontaneous decarboxylation of 7-carboxy-K252c while spontaneous decarboxylation is not possible in the enol tautomer because of the sp^2 hybridized C-7 (Figure 7B). The modeling of FAD into the active site of RebC-10x in the IN conformation reveals that the 7-carboxy group and the pyrrole-ring of the ligand clash with the isoalloxazine of FAD. The steric and electrostatic effects caused by this clash when the FAD conformation is changed from OUT to IN during the substrate binding could be the driving force behind the spontaneous decarboxylation in the StaC-like enzymes. After the decarboxylation, C-7 needs to be protonated by a general acid in order to produce the StaC product K252c. This protonation could be achieved by the ordered water molecule, which is present in the RebC-10x crystal structure in the space created by the lower position of the Arg-230 (Figure 8B). In the case of RebC, the hybridization state of the C-7 would change from sp^2 to sp^3 upon hydroxylation

through the canonical FAD-dependent monooxygenase mechanism, after which the spontaneous decarboxylation could generate the RebC product arcyriaflavin A (Figure 7B) (Goldman et al., 2012).

1.2.4 Lsd18 catalyzes epoxidation reactions in the lasalocid biosynthesis

Ionophore polyethers, like lasalocids and monensin, which are active against Gram-positive bacteria, are polyketides that have a polycyclic ether skeleton with several stereocenters (Dutton et al., 1995, Rutkowski and Brzezinski, 2013) (Figure 9A). The structural diversity of these polyethers is derived from the number and size of the ether rings that are formed by the stereoselective epoxidation of the linear polyene intermediate followed by the regioselective cyclization. Epoxide hydrolase Lsd19 from the lasalocid biosynthetic pathway has been determined to catalyze the formation of the ether rings by anti-Baldwin cyclization (Shichijo et al., 2008, Hotta et al., 2012).

Before the formation of the ether rings, the polyene intermediate has to be epoxidized. This function in the lasalocid pathway has been assigned to FPMO Lsd18 by *in vivo* and *in vitro* experiments with substrate analogues. The biotransformation experiments with *Rhodococcus eryhropolis* L-88 carrying an expression vector of the *lsd18* gene showed that Lsd18 was able to stereoselectively epoxidate several different substrate analogues (Figure 9B and 9C) (Minami et al., 2012).

The *in vitro* experiments with heterologously expressed and purified Lsd18, in the presence of NAD(P)H, FAD and flavin reductase Fre, showed the conversion of the C-12–C-24 diene mimic into monoepoxidated product (Figure 9D). Also, the isolasalocid ketone, which forms during acid treatment of the bisepoxide product, was detected from the reaction mixture, indicating that Lsd18 has catalyzed two consequtive epoxidations. The presence of FAD and Fre were not required for the formation of the monoepoxidated product, but they were shown to enhance the efficiency of the reaction. The addition of Lsd19 to the reaction mixture yielded both the monoepoxidated product and the lasalocid ketone, which has the same modification pattern as lasalocid A. Altogether the results from the biotransformation and *in vitro* experiments demonstrate the ability of the FPMO Lsd18 to catalyze two sequential and enantioselective epoxidation reactions in the biosynthesis of the lasalocid group of polyethers by using the 4a-hydroperoxyflavin in the oxidative half-reaction (Minami et al., 2012).

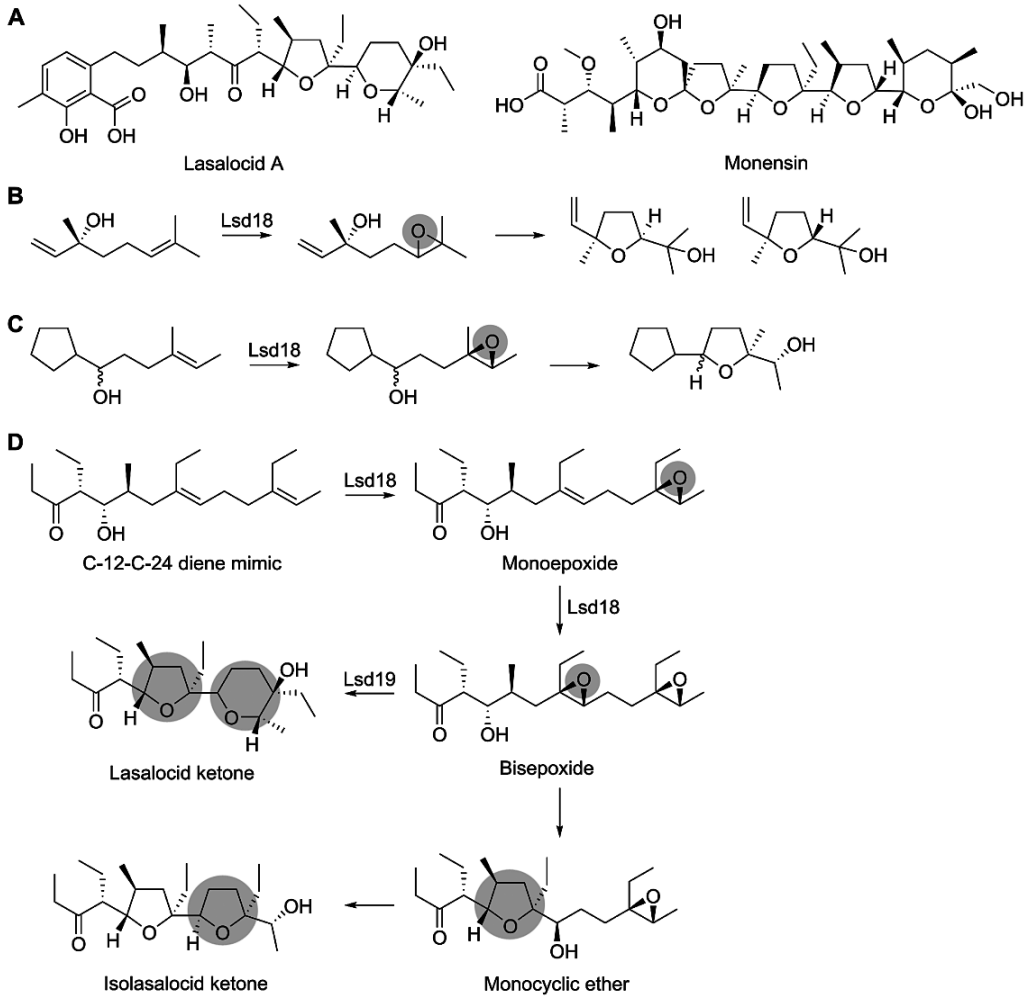

Figure 9: (A) Structures of ionophore polyethers lasalocid A and monensin. (B, C) The epoxidation reactions catalyzed by Lsd18 for different substrate analogues in biotransformation experiments and (D) the sequential epoxidations by Lsd18 and the following ether ring formation by Lsd19 in the conversion of the substrate analogue to lasalocid ketone *in vitro*. Panels B, C and D adapted from Minami et al., 2012.

1.3 Short-chain alcohol dehydrogenases/reductases

Short-chain alcohol dehydrogenases/reductases are a large superfamily of proteins catalyzing several different types of reactions, including oxidoreductions and epimerisations. Members of this superfamily can be recognized by specific amino acid sequences and a similar catalytic mechanism (Kavanagh et al., 2008). These enzymes typically have amino acid sequence identities of only 15–30%, but they are structurally very similar (Jörnvall et al., 1995, Kallberg et al., 2002a). The structure of SDR enzymes is built around a Rossmann fold, which is typical in dinucleotide cofactor binding

enzymes. This fold consists of 6–7 seven β-strands, which makes up the central parallel β-sheet. The β-sheet is flanked by 3–4 α-helices from each side forming the nucleotide binding cavity (Figure 1A in IV and 2A in V). Members of this superfamily have been found in all branches of life and have been shown to be involved for instance in lipid, amino acid, hormone and xenobiotic metabolism (Kavanagh et al., 2008).

The SDR enzymes are divided to six different subfamilies based on their size, conserved amino acid sequences and similar reaction mechanism (Kallberg et al., 2002b, Persson et al, 2009). Two most common subfamilies of SDR enzymes are classical and extended SDR enzymes, which are ~250 and ~350 amino acids long, respectively. The extra ~100 amino acid residues of extended SDR enzymes are located in the C-terminal end of these enzymes and are usually involved in the substrate binding (Kavanagh et al., 2008, Allard et al., 2001a). Three other SDR subfamilies, intermediate, divergent and complex SDR enzymes, are recognized based on specific amino acid sequences, which differ from classical and extended SDR enzymes. Besides amino acid differences, complex SDR enzymes are also parts of large multidomain enzymes (Kallberg et al., 2002b). The sixth SDR subfamily is called atypical and members of this subfamily often are missing the amino acids of the catalytic tetrad. They also have various other sequence differences compared to other SDR enzymes but retain the topology typical for the SDR enzymes (Persson et al., 2009, Link et al., 2012, Buysschaert et al., 2013).

The SDR enzymes involved in the biosynthesis of natural products belong mostly to classical, extended and complex subfamilies. Angucyclinone tailoring enzymes discussed in the experimental section are classical SDR enzymes whereas SDR enzymes involved in the sugar biosynthesis belong to the subfamily of extended SDR enzymes (Allard et al., 2001a, IV). Since the KR domains from the type I PKS are part of large multidomain enzymes, they are classified as complex SDR enzymes (Kavanagh et al., 2008).

1.3.1 Reaction mechanism of the SDR enzymes

The reaction mechanism of the oxidations and reductions of the hydroxyl and keto groups of substrates, respectively, by SDR enzymes has been extensively studied. The canonical reaction mechanism of the classical SDR enzymes has mainly been deduced from kinetic studies with *Drosophila* alcohol dehydrogenase, but also other members of this enzyme family have been shown to follow the same mechanism. The catalytic triad of the SDR enzymes consists of amino acids Ser-Tyr-Lys, where tyrosine is the most conserved amino acid in this enzyme superfamily. In some cases an additional Asn residue is included in this triad, formulating the catalytic tetrad Asn- Ser-Tyr-Lys (Filling et al., 2002).

The reaction catalyzed by the SDR enzymes starts with the binding of the coenzyme NAD(P)H in an extended conformation, followed by the binding of the substrate. The next steps of the catalytic cycle are a proton transfer between the side-chain hydroxyl of tyrosine and the hydroxyl/keto group of the substrate and the following 4-*pro*-S hydride

transfer between the nicotinamide ring of the NAD(P)(H) and the carbon atom of the substrate where the hydroxyl/keto group is attached (Figure 10). After the reaction, the oxidized or reduced product dissociates from the active site prior to the release of the reduced or oxidized coenzyme, respectively (Filling et al., 2002).

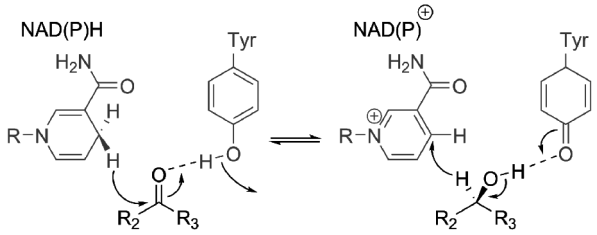

Figure 10: The general reduction and oxidation reactions catalyzed by the SDR enzymes. The proton from the tyrosine in the ketoreduction is transferred to proton relay system, which often involves the 2'-OH of the ribose in NAD(P)H, the side chain of lysine from catalytic triad and water molecule coordinated by the asparagine from the catalytic tetrad. The general keto/hydroxyl substrates are shown in black, NAD(P)H and catalytic tyrosine in grey.

The roles of the different catalytic amino acids are also well known. As described above, the Tyr residue acts as a general acid or base in donating or abstracting a proton to or from the substrate, respectively. The role of the Lys residue adjacent to Tyr is to lower the pK_a value of the Tyr in order to facilitate the action of Tyr as a catalytic acid or base. The Ser residue of the catalytic tetrad is involved in the stabilization and polarization of the substrate hydroxyl/keto group and the Asn residue is important for the formation of the proton relay system between the active site residues and the surrounding solvent molecules (Filling et al., 2002).

1.3.2 Ketoreductases determine the stereochemistry in type I polyketides

One of the most thorough functional and structural characterizations of SDR enzymes involved in the natural product biosynthesis has been done with the KR domains of the modular type I PKSs (Figure 2A) (Caffrey, 2003, Keatinge-Clay, 2007, Whicher et al., 2014). These KRs are responsible for the formation of stereocenters in type I polyketides by catalyzing the reduction of the keto groups into hydroxyl groups with specific stereochemistries during polyketide synthesis. The main goal in the study of these KRs has been in understanding how the stereospecificity of these ketoreductions is controlled. The KRs can be divided into different types based on the stereochemistry of the formed hydroxyl group and their ability to epimerize the growing polyketide chain (Caffrey, 2003, Keatinge-Clay, 2007).

A1-type KRs catalyze the formation of a β-hydroxyl group with an *S* stereochemistry whereas B1-type KRs are responsible for the formation of *R*-β-hydroxyl groups (Figure 2A). A2- and B2-type KRs catalyze the formation of a hydroxyl group with the same stereochemistry as A1- and B1-type KRs, respectively, but they also catalyze the

α-epimerization of the growing polyketide chain. C1-type KRs lack the catalytic tyrosine and are nonfunctional whereas C2-type KRs are ketoreductase-inactive but involved in the epimerization of the α-position (Caffrey, 2003, Keatinge-Clay, 2007). The amino acid residues behind the different stereochemistries of ketoreductions catalyzed by these KRs have been identified as W and LDD motifs in type A and B KRs, respectively. These motifs are responsible for guiding the ACP-tethered polyketide chain into the active site from opposite sides causing the formation of hydroxyl groups with opposite stereochemistries (Caffrey, 2003, Keatinge-Clay and Stroud, 2006, Keatinge-Clay, 2007, Zheng et al., 2010).

1.3.3 The SDR enzymes in the modification of monosaccharides

The SDR enzymes are involved in several different steps in the biosynthesis of the monosaccharide moieties present in natural products. Some of the reactions catalyzed by the SDR enzymes are dehydration, epimerization and ketoreduction (Field and Naismith, 2003). These enzymes are involved in the reaction cascades that typically convert NDP-sugars (NDP = nucleoside diphosphate) into various sugar nucleosides before their attachement to aglycones (Thibodeaux et al., 2008). Most of the sugar moieties observed in natural products are deoxysugars like D-olivose and L-rhodinose present in landomycins and urdamycins, L-daunosamine found in daunorubicin and doxorubicin and D-oliose and D-mycarose present in mithramycins. These sugars are most often derived from the glycolytic intermediates glucose-6-phosphate and fructose-6-phosphate. The first common step in many deoxysugar biosynthetic pathways is the conversion of a sugar-1-phosphate into NDP-sugar, which is then further modified to different sugar nucleosides (Trefzer et al., 1999, Thibodeaux et al., 2008). In the following sections, mechanisms of the different sugar modifying enzymes will be discussed in order to give an overview how various different sugar moieties found in natural products are formed.

1.3.3.1 4,6-dehydratases produces NDP-4-keto-6-deoxy-D-glucose

The first modification reaction of the sugar moiety in most biosynthetic pathways is the conversion of NDP-sugar into the corresponding NDP-4-keto-6-deoxy-sugar. This reaction is a requisite to all downstream modification reactions as the formed 4-keto group activates the C-3' and C-5' protons by lowering their pK_a values. Many of the modification reactions also appear directly at the site of the 4-keto group (Thibodeaux et al., 2008). One of the best studied enzymes to catalyze this conversion is the dTDP-D-glucose (dTDP = thymidine diphosphate) 4,6-dehydratase RmlB from the L-rhamnose biosynthetic pathway (Figure 11). The crystal structures of RmlB from *Salmonella enterica* serovar Typhimurium in complex with NAD^+ (PDB code 1G1A), NAD^+ + dTDP (1KEW) and NAD^+ + dTDP-D-glucose (1KEU) and from *Streptococcus suis* in complex with NAD^+ + dTDP (1KET), NAD^+ + dTDP-D-glucose (1KER) and NADH + dTDP-xylose (1KEP) have given insights into the reaction mechanism of this enzyme (Allard et al., 2001b, Allard et al., 2002).

The reaction catalyzed by RmlB (and also other 4,6-dehydratases) is a three-step process, which involves the oxidation of the hydroxyl group at C-4', dehydration from C-5' and C-6' and the reduction of the double bond between carbons C-5' and C-6' (Figure 11) (Glaser, 1963, Allard et al., 2002). The first oxidation step is catalyzed according to the canonical reaction mechanism of the SDR enzymes involving the catalytic tyrosine residue as a general base and the hydride transfer from substrate to NAD^+. The dehydration of the 4-ketoglucose intermediate is catalyzed by Glu and Asp residues in the active site of the RmlB. The Glu residue acts as a base in abstracting a proton from C-5', and the Asp residue is an acid that protonates the leaving hydroxyl group at C-6' causing the loss of a water molecule. This reaction mechanism has been verified by the structural and mutational analysis of the 4,6-dehydratase DesIV involved in the desosamine biosynthesis in *S. venezuelae* (Allard et al., 2004).

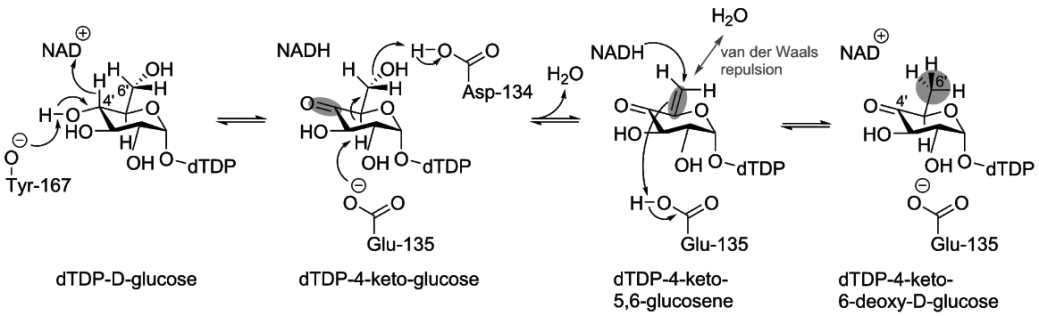

Figure 11: The conversion of dTDP-D-glucose to dTDP-4-keto-6-deoxy-D-glucose by 4,6-dehydratase RmlB from the L-rhamnose biosynthetic pathway. Figure adapted from Allard et al., 2002 and 2004.

The last step in this reaction cascade, which results in the formation of the NDP-4-keto-6-deoxy-D-glucose, utilizes either the catalytical Tyr or the Glu residue involved in the dehydration reaction as an acid to protonate C-5' and NADH to donate a hydride to C-6' (Allard et al., 2002, Allard et al., 2004). The modeling of dTDP-4-keto-5,6-glucosene intermediate to the structure of DesIV positions the catalytic Tyr and Thr-127 within hydrogen bonding distance from 4'-keto group whereas Glu-129 (corresponds to Glu-135 in RmlB) is in cloce vicinity of C-5'. This vicinity is required for the proton transfer reaction to occur. This modeling suggests that the Glu residue involved in the dehydration reaction is also involved in the last reduction step of this reaction cascade (Allard et al., 2004). In order to correctly position the dehydrated substrate for the reduction step, conformational changes bringing the C-6' of the substrate into vicinity of the NADH are required. These changes have been proposed to occur due to a steric hindrance between the C-6' and the water molecule resulting from the dehydration reaction (Allard et al., 2002, Allard et al., 2004) This hypothesis is supported by the finding of coordinated water molecule at the position of the glucosyl 6'-hydroxyl group in the structure of *S. suis* RmlB in complex with NADH and dTDP-xylose. This shows that the water

molecule lost during the dehydration reaction can be trapped within the active site to enable the conformational changes in the substrate, which are required for the reduction reaction to occur (Allard et al., 2002).

1.3.3.2 Ketoreductions generate hydroxyl groups in sugar nucleotides

SDR enzymes involved in sugar biosynthesis are also involved in generating hydroxyl groups by catalyzing ketoreductions of different positions. One of the possible reasons for the high number of ketoreductases observed in deoxysugar biosynthesis may be the need to stabilize the NDP-sugars after necessary modifications by reducing the activating C-4' keto groups from the structures (Figure 12) (Thibodeaux et al., 2008). The reduction of the activating keto into a hydroxyl group reduces the activity of the sugar by lowering the acidity of the protons at positions C-3' and C-5' and hence lowers the reactivity of positions C-3', C-5' and C-6' (Blankenfeldt et al. 2002, Thibodeaux et al., 2008).

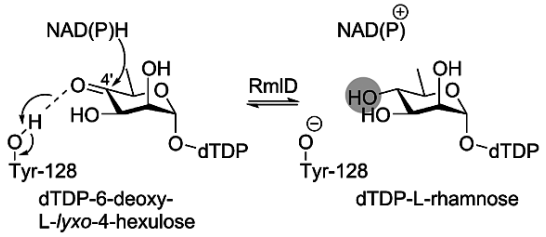

Figure 12: The 4-ketoreduction of dTDP-6-deoxy-L-*lyxo*-4-hexulose to dTDP-L-rhamnose by RmlD from the L-rhamnose biosynthetic pathway. Figure adapted from Blankenfeldt et al., 2002.

The reaction mechanism of the ketoreductions follows the canonical reaction mechanism of the SDR enzymes. One well-studied example is from the biosynthesis of L-rhamnose, where RmlD catalyzes the last step of the pathway: the conversion of dTDP-6-deoxy-L-*lyxo*-4-hexulose to dTDP-L-rhamnose (Figure 12) (Graninger et al., 1999). The 4-ketoreduction in L-rhamnose formation requires a proton transfer between the hydroxyl group of the active site tyrosine and the keto group of the substrate as well as a hydride transfer from the NADPH to the C-4' carbon of the sugar moiety. These distances in the crystal structure of RmlD in complex with NADPH + dTDP-L-rhamnose (PDB code 1KC3) are 3.9 and 3.1 Å, respectively, indicating that proton and hydride transfers are possible.

The biggest difference between RmlD and many other SDR enzymes is that, instead of serine, there is threonine residue as part of the catalytic triad in the active site. The conserved nature of Ser to Thr change still enables the hydrogen bonding between the Thr residue and the carbonyl group of the substrate. This interaction is important for the lowering of the pK_a value of the carbonyl moiety, which is required for the activity of the SDR enzymes (Blankenfeldt et al., 2002).

1.3.3.3 Epimerases act in different positions on the sugar nucleotides

The purpose of epimerases is to create versatility into the sugar moieties by changing the stereochemistry of the carbon atoms. Epimerases can catalyze the epimerization of one or two carbons at the same time, and epimerization activities can be coupled to reductions or oxidations of the keto or hydroxyl groups, respectively (Figures 13 and 14) (Thibodeaux et al., 2008). These oxidation and reduction reactions in epimerases follow the canonical mechanism of the SDR enzymes (Allard et al., 2001a, Thibodeaux, et al., 2008).

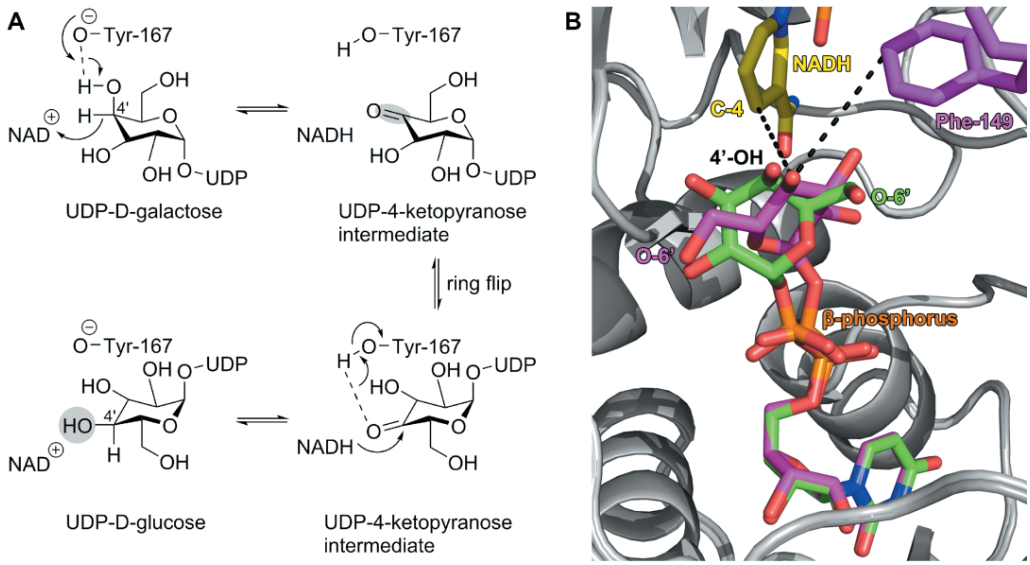

Figure 13: (A) The conversion of UDP-galactose into UDP-glucose in the epimerization reaction catalyzed by GALE. The ring flip of the UDP-4-ketopyranose intermediate changes the orientation of the C-4' between Tyr-167 and NAD(H) to enable the proton and hydride transfer from opposite sides of UDP-D-galactose and UDP-D-glucose during the epimerization. Figure adapted from Thoden and Holden, 1998 and Frey and Hegeman, 2013. (B) A close-up views from the active site of *E. coli* GALE Y149F/S124A variant in complex with NADH + UDP-galactose (violet) (PDB code 1A9Z) and NADH + UDP-glucose (green) (1A9Y). NADH (yellow) and Phe-149 (violet) from complex structure with UDP-galactose are shown as stick models and their possible connections with 4'-hydroxyl of UDP-galactose as black dashed lines.

The epimerization of UDP-galactose (UDP = uridine diphosphate) into UDP-glucose by UDP-galactose-4-epimerase (GALE) takes place through oxidation of the 4'-hydroxyl group followed by a ring flip, which makes it possible for the NADH to donate the 4-*pro*-S hydride to the opposite side of the sugar ring than where it was removed from during the oxidation (Figure 13A) (Frey and Hegeman, 2013). The changes in the conformation of the sugar can be seen from the crystal structures of the inactive *E. coli* GALE Y149F/S124A variant in complex with NADH + UDP-galactose (PDB code 1A9Z) and NADH + UDP-glucose (1A9Y) (Figure 13B). These structures show

that the differences in the conformation of UDP-galactose and UDP-glucose start from the β-phosphorus atom and result in a flip of the sugar ring. This flip positions the 4'-hydroxyl groups with different stereochemistries into the same position, indicating that it is possible to reduce the keto groups into either one of the epimers (Thoden and Holden, 1998).

Epimerization reactions catalyzed by GDP-fucose (GDP = guanosine diphosphate) synthase (GFS) and GDP-mannose-3',5'-epimerase (GME) involve a more complex reaction mechanism than the one utilized by GALE (see above). GFS catalyzes the epimerization of C-3' and C-5' positions followed by the reduction of C-4' (Figure 14A) (Lau and Tanner, 2008). In contrast, GME converts GDP-D-mannose into GDP-L-galactose and GDP-L-gulose by catalyzing oxidation of C-4' followed by epimerization of both C-3' and C-5' or just C-3', respectively (Figure 14B) (Major et al., 2005). The final step in both routes is reduction of C-4' back to a hydroxyl group (Major et al., 2005, Lau and Tanner, 2008). The substrate for GME is GDP-D-mannose whereas the substrate for GFS is GDP-6-deoxy-4-keto-D-mannose, the product of the GDP-D-mannose-4,6-dehydratase (catalyzes similar reaction as RmlB in section 1.3.3.1) (Major et al., 2005, Lau and Tanner, 2008).

The reaction cascade catalyzed by GFS starts with the deprotonation of C-3' by the catalytic base Cys-109 followed by the protonation C-3' by the catalytic acid His-179 from the opposite side of the substrate (Figure 14A). The formed GDP-6-deoxy-4-keto-altrose is deprotonated and protonated from position C-5' by the same residues leading to the formation of GDP-6-deoxy-4-keto-L-galactose, which is then reduced into GDP-L-fucose (Lau and Tanner, 2008).

A highly similar reaction cascade catalyzed by GME starts with the oxidation of 4'-hydroxyl and is followed by deprotonation and protonation of position C-5' by the catalytic amino acid residues Cys-145 and Lys-217, respectively, corresponding to residues Cys-109 and His-179 in GFS, respectively (Figure 14B). These reactions are followed by a ring flip, similar to the one in the GALE reaction, and produce an intermediate product GDP-4-keto-L-gulose. This intermediate is then reduced into GDP-L-gulose or converted into GDP-L-galactose. The conversion into galactose requires a change in the conformation of the sugar ring either by a ring flip similar to the one above or by movement of the C-4'. The most likely explanation is the movement of C-4', which transfers GDP-4-keto-glucose to a boat conformation by moving the C-4' through the plane of the ring. After this conformational change, the deprotonation and protonation of position C-3' by Cys-145 and Lys-217, respectively, produces an half chair intermediate, which changes back to the previous conformation. The final step of the reaction cascade is the reduction of position C-4' into the hydroxyl group present in GDP-L-galactose (Major et al., 2005).

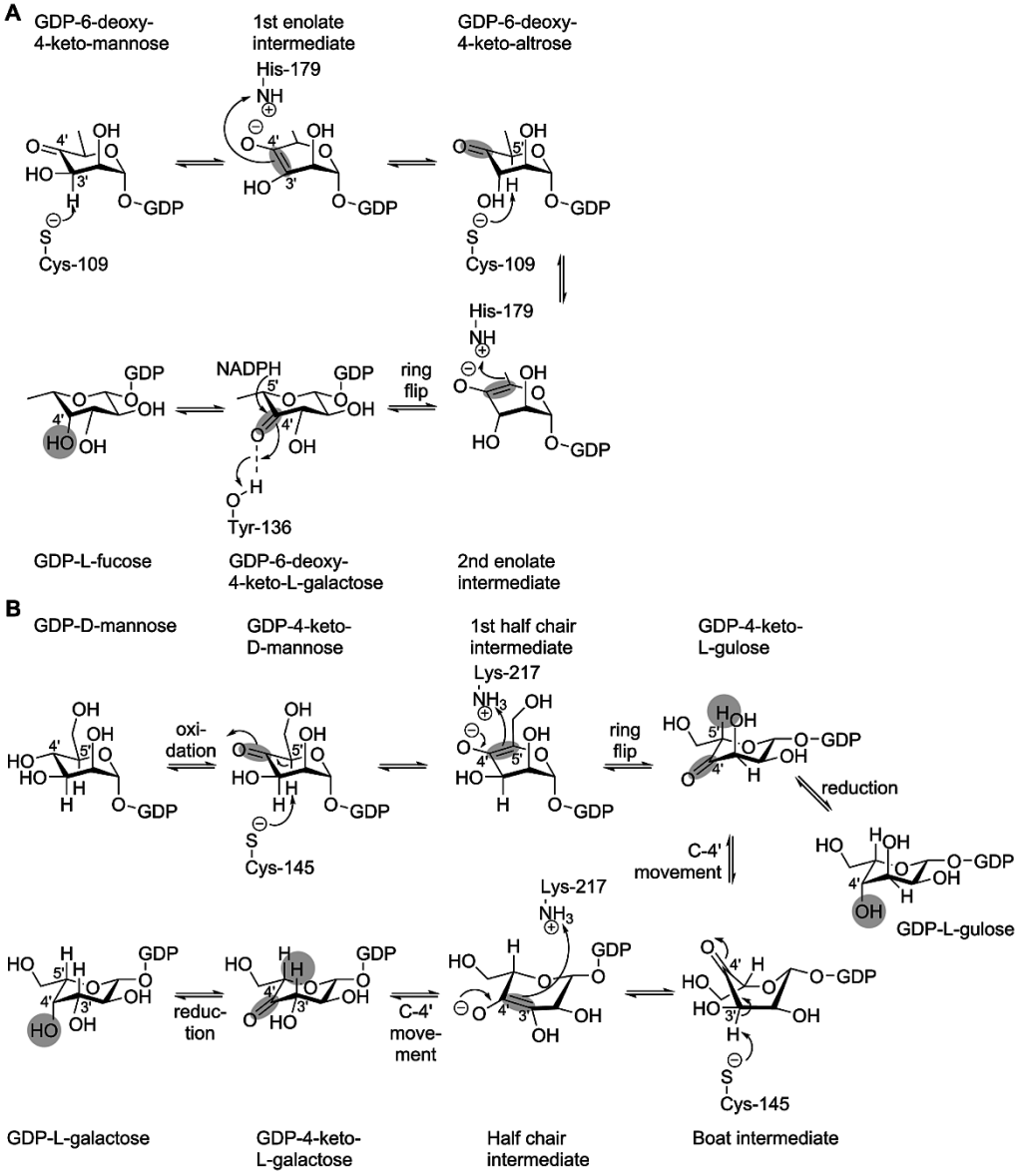

Figure 14: (A) The conversion of GDP-4-keto-6-deoxy-D-mannose to GDP-L-fucose by GFS and (B) the conversion of the GDP-D-mannose into GDP-L-galactose and GDP-L-gulose by GME. The oxidation and reduction reactions in panel B are catalyzed with the canonical SDR reaction mechanism using Tyr-174 and NAD(H). In order to simplify the figure, only protons involved in the catalytical steps are shown. Panel A adapted from Lau and Tanner, 2008 and panel B from Major et al., 2005.

1.3.4 Srm26 catalyzes ketoreduction in the biosynthesis of spiramycin

One of the several different SDR enzymes suggested to catalyze ketoreductions in the biosynthesis of natural products is Srm26. *In vivo* experiments have shown that this

enzyme is involved in the generation of the hydroxyl group at C-9 of the spiramycin macrolactone ring. The inactivation of the *srm26* gene from the spiramycin producer *Streptomyces ambofaciens* OSC2 resulted in the accumulation of platenolide I, a metabolite bearing a keto group at position C-9 (Figure 15). The production of spiramycins I, II and III in *srm26*-deficient *S. ambofaciens* could be restored by introducing a plasmid containing the *srm26* gene into the strain. These results show that Srm26, a potential member of the atypical SDR enzyme family, catalyzes a ketoreduction reaction typical to SDR enzymes (Nguyen et al., 2013).

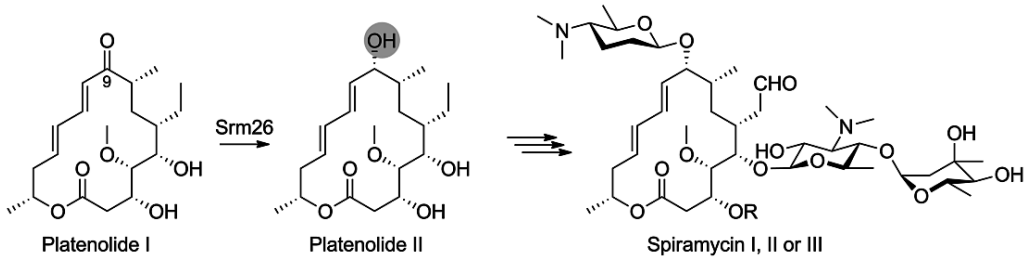

Figure 15: The 9-ketoreduction of platenolide I catalyzed by Srm26 and the structures spiramycins I, II and III. R = H in spiramycin I, $COCH_3$ in spiramycin II and $COCH_2CH_3$ in spiramycin III. Figure adapted from Nguyen et al., 2013.

1.3.5 Gra-ORF6 acts in the branching point of benzoisochromanequinones

Benzoisochromanequinones (BIQ) are aromatic type II polyketides that are built around a three-ring system composed of pyran, quinone and benzene rings. The biosynthesis of these metabolites proceeds through a common bicyclic intermediate after which different tailoring enzymes catalyze the reactions responsible for the formation of distinct BIQ scaffolds (Taguchi et al., 2001, Metsä-Ketelä et al., 2013). In the biosynthetic pathways of actinorhodin and granaticin, the bicyclic intermediate is converted to the first chiral intermediate, 4-dihydro-9-hydroxy-1-methyl-10-oxo-3-*H*-naphtho[2,3-*c*]pyran-3-acetic acid (DNPA), with either *S* or *R* stereochemistry at C-3 position, respectively (Figure 16). The differing stereochemistries at this position are due to the different strereochemistries of the 3-hydroxyl groups in the preceding intermediate, which goes through cyclization into the hemiketal form followed by dehydration into DNPA (Taguchi et al., 2004).

In actinorhodin biosynthesis, ActVI-ORF1 (ORF = open reading frame) has been shown to catalyze the 3-ketoreduction of the bicyclic intermediate by *in vivo* experiments. The expression of the *actVI*-ORF1 gene together with the actinorhodin minimal PKS, aromatase, cyclase and 9-ketoreductase genes resulted in the production of (*S*)-DNPA (Ichinose et al., 1999). In similar experiments with genes from the granaticin pathway, *gra*-ORF5 was enough to complement actinorhodin 9-ketoreductase *act*III. The production of (*R*)-DNPA in high amounts required translational coupling of *gra*-ORF5

and *gra*-ORF6 genes in the production plasmid. These genes are translationally coupled also in the granaticin producing strain *Streptomyces violaceoruber* Tü22 (Taguchi et al., 2001, Sherman et al., 1989).

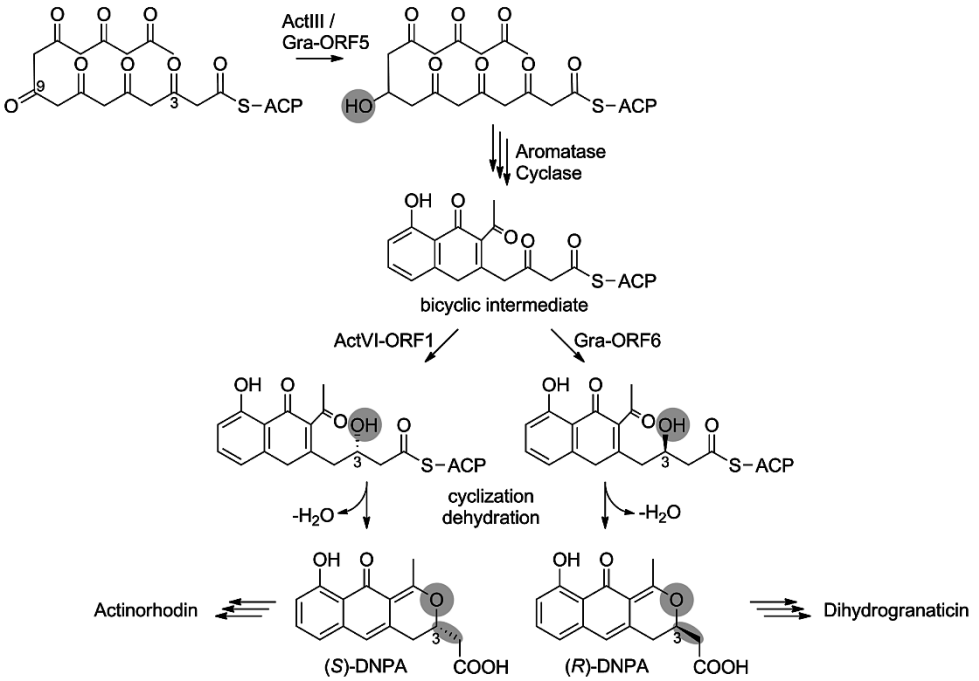

Figure 16: The conversion of the bicyclic BIQ intermediate to either (*S*)- or (*R*)-DNPA by ActVI-ORF1 and Gra-ORF6 from the actinorhodin and granaticin biosynthetic pathways, respectively. The 9-ketoreduction of the linear octaketide produced by the minPKS is catalyzed by ActIII or Gra-ORF5 and the bicyclic intermediate is formed after aromatization and cyclization reactions. Figure adapted from Taguchi et al., 2001 and Taguchi et al., 2004.

Although ActVI-ORF1 and Gra-ORF6 catalyze the same reaction with opposite stereochemistry for the same substrate, based on the sequences they belong to different enzyme families; ActVI-ORF1 is a 3-hydroxyacyl-CoA dehydrogenase whereas Gra-ORF6 is an SDR enzyme (Taguchi et al., 2001). The homology model structure of Gra-ORF6 in complex with NADPH has shown that all the amino acids of a classical catalytic triad of the SDR enzymes are present in the active site of Gra-ORF6 and are in the vicinity of NADPH, which is positioned correctly to donate the 4-*pro*-S hydride to the bicyclic substrate (Taguchi et al., 2004). These results suggest that Gra-ORF6 is a classical SDR enzyme catalyzing a stereospecific 3-ketoreduction of the bicyclic intermediate and is responsible for the diversion of the granaticin pathway from other BIQ pathways.

2. AIMS OF THE STUDY

The aim of this PhD project was to study the mechanisms behind the functional differentiation of angucyclinone tailoring enzymes. These enzymes are responsible for the production of different angucycline metabolites in jadomycin (*jad*), landomycin (*lan*), urdamycin (*urd*) and gaudimycin (*pga* and *cab*) pathways. The first goal was to find out enzymes responsible for the biosynthetic steps behind the evolution of these metabolites. The second goal of this study was to use protein X-ray crystallography and mutagenesis to analyze these homologous enzymes more carefully and to pinpoint the exact amino acid residues behind their different functions. Overall, the aim of this study was to gain more information about the biosynthesis of angucyclines and to improve our possibilities to use these biosynthetic enzymes as tools for producing novel angucycline metabolites.

The specific aims of this study were:

- To produce and purify the angucycline tailoring enzymes and study their reactions
- To solve the crystal structures of tailoring enzymes behind the differentiation of angucycline biosynthetic pathways
- To analyse structure-based sequence alignment in order to find out which amino acids are different between these homologous tailoring enzymes
- To find out amino acid regions responsible for the different activities of angucycline tailoring enzymes by analyzing the properties of chimeric enzymes

3. SUMMARY OF THE MATERIALS AND METHODS

3.1 Cloning and mutagenesis of the biosynthetic genes

The biosynthetic genes used in this study were amplified with Phusion DNA polymerase using chromosomal DNA of *Streptomyces* sp. H021 (Palmu and Kunnari, 2002) (*cabV*) (I) and *S. fradiae* AO (Trefzer et al., 2001) (*urdE*, *urdM*, *urdMox* and *urdMred*) (II) or cosmid H2-26 (Westrich et al., 1999) (*lanE* and *lanV*) (II) as a template. For the heterologous production of the biosynthetic enzymes, the amplified genes were subcloned into the pBHBΔ plasmid (Kallio et al., 2006) as *Bgl*II/*Hin*dIII fragments, and the constructs were verified by analytical digestion and sequencing (Eurofins MWG Operon) (I, II). The revised nucleic acid sequences of *lanE* and *urdM* were deposited to GenBank under accession numbers JQ782417 and JQ782418. The mutagenesis of the biosynthetic genes was carried out using a modified four-primer overhang extension polymerase chain reaction (PCR) method (Ho et al., 1989), and the mutated genes were subcloned to pBHBΔ and verified as above (III–V).

3.2 Production and purification of the enzymes

To study the activities of these biosynthetic enzymes, they were heterologously produced in *Escherichia coli* TOP10 strain as polyhistidine-tagged proteins. The purified proteins carried an N-terminal (M)AHHHHHHHRS-sequence derived from the expression plasmid, and the purification was carried out using Ni^{2+}- or Co^{2+}-affinity chromatography using imidazole to elute the resin bound proteins (I-V). For the crystallization trials, enzymes were desalted or further purified with a PD-10 column (GE Healthcare) or by size exclusion chromatography on a HiLoad Superdex200 26/600 preparative grade column (GE Healthcare), respectively. The proteins were concentrated with Centriprep and Amicon Ultra devices (Millipore) (III–V). The purity of the enzymes was confirmed with sodium dodecyl sulfate-polyacrylamide gel electrophoresis (SDS-PAGE), and the protein concentration was estimated using the Bradford dye method (Bradford 1976) (I–V), NanoOrange Protein Quantitation Kit (Invitrogen) (I) or NanoDrop 2000 (Thermo Scientific) at 280 nm (IV, V). To analyze the oligomerization of the enzymes, gel filtration analysis was performed by HPLC (Shimadzu VP series chromatography system with a diode array detector, SPD-M10Avp, Tosoh Biosciences TSKgel SuperSW2000/4.0 μm column, isocratic run with 100 mM potassium phosphate buffer, pH 7.6, flow rate 0.16 ml/min) (IV). The enzymes purified and used in this study were JadH, LanE, UrdE, PgaE, CabE, LanV, CabV, LanM2, UrdM and UrdMred (the reductase domain of UrdM produced and purified separately from the oxygenase domain).

3.3 Production and purification of substrates

The substrate prejadomycin for the *in vitro* reactions was obtained from cultures of *Streptomyces lividans* TK24/pMC6BD strain (Metsä-Ketelä et al., 2003) grown at +30 °C for 7 days in shaking in E1 media with 20 g/l XAD-7 resin as an absorbent and 10 µg/ml thiostrepton. The XAD-7 resin was collected from the culture broth by decanting and water washes. The bound metabolites were extracted with methanol, followed by chloroform extraction in acidic conditions and several repeated washes with water. The compounds were resolubilized in methanol and purified using preparative scale reverse-phase HPLC (RP-HPLC). The main fractions were collected, extracted with chloroform and further purified with selective crystallization from methanol. The purified substrate was redissolved in methanol for storage and use in the *in vitro* reactions (I–V).

The substrate 12-hydroxy-prejadomycin was produced *in vitro* from prejadomycin in the presence of PgaE and NADPH. The reaction was carried out with NADPH concentration sufficient for PgaE to 12-hydroxylate all prejadomycin but not to catalyze the 12b-hydroxylation. Reaction products were bound to a pre-equilibrated solid-phase extraction (SPE) column (Discovery DSC-18, Supelco), eluted with methanol and used immediately as a substrate for the enzymatic *in vitro* reactions (I–III).

3.4 Analysis of enzymatic reactions

Enzymatic reactions were carried out in 100 mM potassium phosphate buffer pH 7.6 at room temperature. The volumes ranged from 200 µL to 1 mL depending on the application. The consumption of NADPH in the reactions was detected as a decrease of fluorescence (excitation 355nm / emission 460nm) (I, II). The consumption of the substrates prejadomycin or 12-hydroxy-prejadomycin was detected spectrophotometrically at 406 nm or 510 nm, respectively (I–III). The reaction products were extracted with repeated chloroform extractions or analytical scale SPE columns and resolubilized or eluted, respectively, in methanol for RP-HPLC analysis (Kallio et al., 2008a). The RP-HPLC analysis of the extracted reaction products was conducted with C-18 RP-HPLC column using gradient from 15% acetonitrile + 0.1% formic acid to 100% acetonitrile (I–V).

The liquid chromatography-mass spectrometry (LC-MS) analysis of the substrate and products was conducted with a Micromass Quattro Premier tandem quadropole mass spectrometer (Waters Corp.) using positive electrospray ionization (ESI) connected to an equivalent RP-HPLC system as used above (I, IV). The high-resolution mass analysis was conducted with a micrOTOF-Q mass spectrometer (Bruker Daltonics) using negative ESI connected to a RP-HPLC system equivalent to the one used above (II).

The anaerobic conditions required to study the oxygen dependence of FPMOs were achieved using a Thunberg cuvette connected to a vacuum and a nitrogen source, aided by brief ultrasound bath treatments or a glucose oxidase/catalase treatment (Fabian, 1965) (I, II). The incorporation of ^{18}O to the products from molecular oxygen

or water was achieved by addition of 99% $^{18}O_2$ or 50–75% (v/v) $H_2{}^{18}O$, respectively, to the reaction mixture in Thunberg cuvette (I). To study the use of NADPH in the LanV reaction, coupled reactions of PgaE and LanV using prejadomycin as a substrate were conducted with deuterium-labeled NADPH. The 4-*pro*-S labeled NADP^{2}H was prepared *in vitro* with glucose dehydrogenase from *Bacillus megaterium* (Podschun et al., 1993) (IV).

3.5 Kinetic analysis of the PgaE variants

The kinetic analysis of the different PgaE variants was carried out by following the consumption of the substrates prejadomycin and 12-hydroxy-prejadomycin spectrophotometrically at 406 nm and 510 nm, respectively, in the presence of the enzyme and NADPH. Prejadomycin was used as a substrate for studying the C-12 hydroxylation and 12-hydroxy-prejadomycin to study the C-12b hydroxylation (III).

Because of the uncertainty in initial rates (~1 min reaction time) of prejadomycin consumption by PgaE, nonlinear parts of the conversion curves (10–15 min reaction time) were fitted to various rate models using numerical integration capabilities of Scientist 2.01 (Micromath, St. Louis, USA). Although these models were consistent with the obtained data, inaccurate reaction rate determination below 10 μM substrate concentration caused considerable flexibility in parameter values. The use of structural and experimental considerations allowed us to fit the parameters on the basis of the following assumptions: (i) one monomer of the PgaE dimer is unlikely to have more than one active site and (ii) mutagenesis experiments revealed amino acids affecting substrate inhibition in the active site and in the dimerization interface. These suggest that the substrate inhibition effect is caused by allosteric interactions between the active sites within the PgaE dimer. Based on these considerations, the obtained kinetic data were analyzed with a model that assumes the independent binding of prejadomycin to the active sites of the monomers within the dimer and V_{SE2} (reaction rate when prejadomycin is present in both monomers) being lower than V_{ES} (reaction rate when prejadomycin is present only in one monomer) (III).

3.6 Structure determination of the PgaE P78Q/I79F, LanV and UrdMred

To obtain more information about the biosynthetic enzymes, their crystal structures were solved. Enzymes were crystallized and the diffraction data for the crystals was collected at the European Synchrotron Radiation Facility (Grenoble, France). The structures were determined by molecular replacement (III–V). The crystallographic coordinates and structure factors of the complex structures PgaE P78Q/I79F + FAD (PDB code 4ICY), LanV + $NADP^+$ (4KWH), LanV + $NADP^+$ + 11-deoxylandomycinone (4KWI), LanV + $NADP^+$ + rabelomycin (4OSO) and UrdMred + $NADP^+$ + rabelomycin (4OSP) have been deposited in the PDB.

3.7 Molecular modeling of the angucyclinones

In order to study the different conformations of angucyclines and their orientation in the active sites of the tailoring enzymes, their structures were modeled by density functional theory (DFT) quantum chemical calculations and geometry optimized using M06-2X hybrid meta-density functional theory with the 6-31G(d) basis set. The calculations were performed using Gaussian09 (version A.01) (Frisch et al., 2009) and analyzed with GUIs GaussView (version 3.07) or (version 5.0.8) (Dennington et al., 2009) and GaussSum (version 2.2) (O'Boyle et al., 2008). All the calculations were performed in the gas phase (II, V).

3.8 ECD spectroscopic measurements and calculation of the ECD spectra

The electronic circular dichroism (ECD) spectra of the compounds were measured in methanol with a 0.1 cm or 1.0 cm path-length cell. The measuring range was from 190 nm or 200 nm to 650 nm at 23 °C or 25 °C, respectively. The ECD spectra were calculated for the molecular models at the same level of theory as they were modeled and by using 24 excited states of the single molecule (II, V). The measured and calculated ECD spectra were used to determine the absolute stereochemistries of different angucyclinones (II). The measured ECD spectra were also used to distinguish between 6*R*- and 6*S*-11-deoxylandomycinones, which cannot be separated by RP-HPLC analysis (V).

3.9 Docking experiments with PgaE, LanV and UrdMred

To study the binding of ligands prejadomycin, 11-deoxylandomycinone and gaudimycin C into the active sites of PgaE, LanV and UrdMred, docking experiments were conducted with GOLD docking tool (Jones et al., 1997) within the Discovery Studio platform (Accelrys Software). Prior to docking, the ligand rabelomycin was removed from the complex structures of LanV and UrdMred with $NADP^+$ and rabelomycin (PDB codes 4OSO and 4OSP). To test the requirement of a coordinated water molecule between NADPH and Tyr-160 of LanV in the presence of 11-deoxylandomycinone, the water molecule was positioned in the active site as in the ternary structure of LanV in complex with NADPH and 11-deoxylandomycinone (4KWI). The used radius of the input-site sphere for the receptor-ligand interaction was 12 Å, which covers the entire active site. The used poses were chosen by the GOLD score values and, in the case of LanV and UrdMred, based on the alignment of the ligand with the catalytic Tyr-160 and $NADP^+$. The ligand prejadomycin was modeled using PRODRG server (Schuttelkopf and van Alten, 2004) whereas the ligands 11-deoxylandomycinone and gaudimycin C were modeled as in section 3.7 (III, V).

4. RESULTS AND DISCUSSION

4.1 Enzymatic reactions (original publications I–II)

The enzymes used in this study originate from five different angucycline pathways: jadomycin (*jad*) (Han et al., 1994, Chen et al., 2005), landomycin (*lan*) (Westrich et al., 1999), urdamycin (*urd*) (Decker & Haag 1995, Faust et al., 2000) and gaudimycin (*pga* and *cab*) (Palmu et al., 2007) pathways. These tailoring enzymes are NADPH-dependent FPMOs (JadH, LanE, UrdE, PgaE and CabE), SDR enzymes (LanV and CabV) or fusion proteins with both two domains (LanM2, UrdM and PgaM). The proteins are highly conserved between different pathways in regards to the genetic organization and amino acid sequence (Figure 2 in II). Previously it has been shown that PgaE catalyzes the formation of an unstable reaction intermediate from prejadomycin in the presence of NADPH and molecular oxygen. Under the same conditions, a coupled reaction of PgaE and PgaM converts prejadomycin to a stable reaction product gaudimycin C in a cascade of reactions (Figure 17) (Kallio et al., 2008a). PgaM has been shown to be a two-domain FPMO/SDR enzyme with an internal start codon between the domains. The presence of the internal start codon results in the production of both full-length PgaM with both domains and the production of only the C-terminal SDR domain (Kallio et al., 2008b). The recovery of UrdMred from the production culture of UrdM and the sequence analysis of UrdM suggested that this enzyme is produced in a similar manner to PgaM, as a full-length protein and an independent SDR enzyme from an internal start codon (II). JadH has also been shown to utilize prejadomycin as a substrate in a reaction that produces CR 1 which spontaneously oxidizes to dehydrorabelomycin (Figure 17) (Chen et al., 2010). Prejadomycin has been suggested to result from the simultaneous release and dehydration of UWM6 from ACP by LanM2, a two-domain FPMO/SDR enzyme from the landomycin pathway (Kharel et al., 2012).

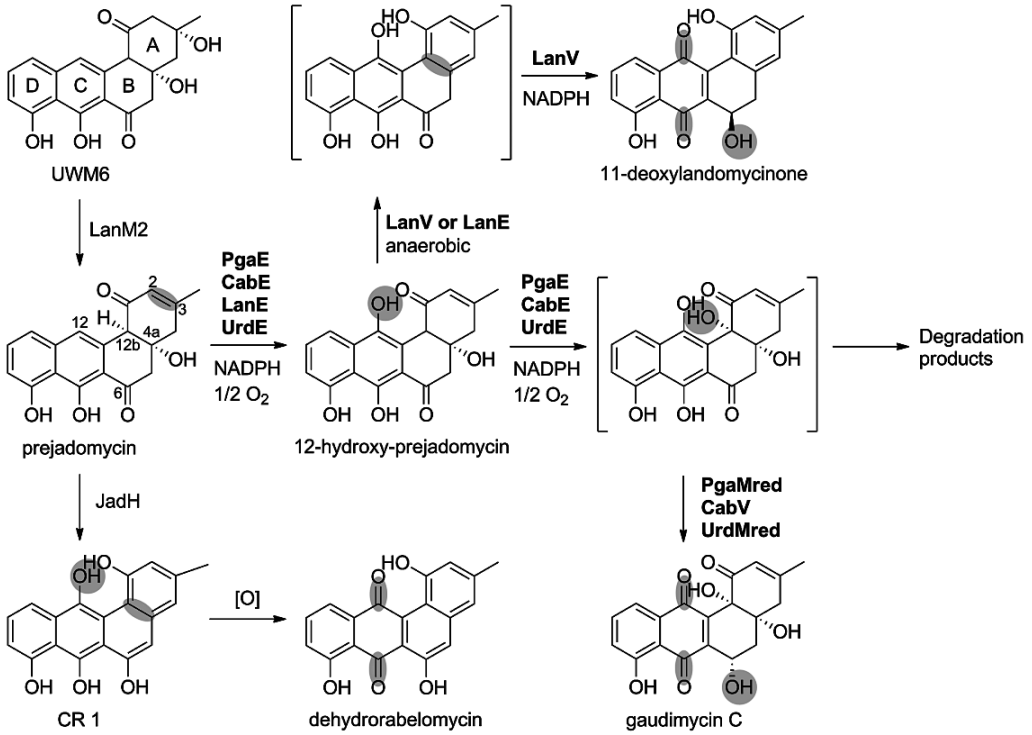

Figure 17: The proposed tailoring reactions in the *pga*, *cab*, *lan*, *urd* and *jad* pathways during the conversion of UWM6 to angucyclinones gaudimycin C, 11-deoxylandomycinone and dehydrorabelomycin. The functions of enzymes presented in bold have been deduced in this study *in vitro* using prejadomycin or 12-hydroxy-prejadomycin as a substrate.

4.1.1 Reactions catalyzed by NADPH-dependent flavoprotein monooxygenases

The NADPH-dependent FPMOs LanE, UrdE, PgaE and CabE, which have been proposed to catalyze C-12 hydroxylation (Faust et al., 2000, Koskiniemi et al., 2007, Palmu et al., 2007), can all consume prejadomycin in the presence of NADPH and molecular oxygen. HPLC analysis shows that no stable product is formed in these reactions but only hydrophilic degradation products can be observed. The comparison of prejadomycin and NADPH consumption in these reactions revealed that NADPH consumption continued even after the depletion of prejadomycin. This observation suggested that the monooxygenases could catalyze two consecutive reactions, which both require the presence of NADPH. These two reactions can clearly be observed in the spectrophotometric analysis where a signal at 510 nm first increases during the consumption of prejadomycin but starts to decrease after prejadomycin depletion (Figures 1 and 2 in I, Figure S2 in II) (I, II).

The separation of these two consecutive reactions was achieved by titration of the NADPH concentration to an amount needed for the complete consumption of prejadomycin. The reactions conducted in limiting NADPH conditions stalled after

all prejadomycin was consumed and the reaction mixtures remained red, consistent with the increase of the 510 nm signal. The addition of NADPH restarted the reactions which then proceeded to completion. The red reaction intermediate could be extracted with C-18 SPE columns and eluted with methanol. After the elution, the extracted reaction product could be used as a substrate by all the monooxygenases LanE, UrdE, PgaE and CabE in the presence of NADPH and O_2 (Figure 2 in I, Figure 5 in II) (I, II). Structural analysis of this extracted reaction intermediate was not possible due to the unstable nature of the compound as it readily degraded within minutes or hours and remained undetectable in RP-HPLC and LC-MS analysis. However, this product was shown to spontaneously convert to dehydrorabelomycin during the RP-HPLC analysis (Figure 1 in I) (I).

The kinetic analysis of PgaE using prejadomycin as a substrate revealed that the consumption of prejadomycin by PgaE was affected by substrate inhibition. The results from the kinetic measurements with the extracted product of the PgaE reaction as a substrate were best fitted with a sigmoidal relationship (Figure 5 in I). These kinetic analyses revealed a clear difference between these two consecutive reactions catalyzed by PgaE as no signs of substrate inhibition were observed during the 12b-hydroxylation (see section 4.2 for details) (I, III).

4.1.2 Reactions catalyzed by the SDR enzymes

The activities of the SDR enzymes CabV, UrdMred and LanV were tested in a coupled reaction with PgaE. The exchange of PgaM to CabV or UrdMred had no effect on the outcome of the reaction, but gaudimycin C was still produced (Figure 17). These results suggested that the oxygenase domains of PgaM or UrdM are not required for the conversion of prejadomycin to gaudimycin C. The formation of gaudimycin C was also achieved when PgaE was replaced with any of the other monooxygenases, LanE, UrdE or CabE. The extracted red reaction intermediate produced from prejadomycin by the monooxygenases could also be converted to gaudimycin C by any combination of the monooxygenases LanE, UrdE, PgaE or CabE and the reductases CabV or UrdMred (Figure 1 in I, Figures 3 and 5 in II) (I, II).

The coupled reactions of LanE, UrdE, PgaE or CabE and LanV converted prejadomycin into a previously unidentified product (Figure 3 in II) (II). The LC-MS and UV-vis (ultraviolet-visible) properties of this compound were identical with 11-deoxylandomycinone (Shaaban et al., 2011), a known intermediate from the landomycin pathway (Figure 17). The structure of this reaction product was confirmed as 11-deoxylandomycinone by electrospray ionization-high-resolution mass spectrometry (ESI-HRMS) and by comparison to an authentic standard using HPLC and ECD spectroscopy (Figure S2 in II) (II).

HPLC analysis of substrate consumption and product formation in the coupled reactions with the monooxygenases and CabV or UrdMred with different NADPH concentrations

revealed a clear separation of two reaction phases. The formation of gaudimycin C was not detected until almost all prejadomycin was consumed (Figure 3 in I, Figure 4 in II) (I, II). However, a similar analysis with monooxygenases and LanV showed no signs of this kind of temporal separation but the formation of 11-deoxylandomycinone was detected immediately after the start of the reaction (Figure 4 in II) (II).

4.1.3 Differences between the biosynthesis of gaudimycin C and 11-deoxylandomycinone

The structure of gaudimycin C suggests that the two reactions catalyzed by the monooxygenases LanE, UrdE, PgaE and CabE are hydroxylations at positions C-12 and C-12b and that the reductases are responsible for 6-ketoreduction (Figure 17). In the biosynthesis of 11-deoxylandomycinone, 12-hydroxylation and 6-ketoreduction are catalyzed by the monooxygenases LanE, UrdE, PgaE and CabE and the reductase LanV, respectively. The exact enzyme catalyzing 4a,12b-dehydration has remained elusive since the separation of reactions catalyzed by LanV and the monooxygenases after 12-hydroxylation has not been successful and since enzymes belonging to both of these families have been shown to catalyze dehydration reactions: SDR enzymes in the biosynthesis of sugar nucleotides and monooxygenases like JadH in the biosynthesis of dehydrorabelomycin (see section 4.2 for other JadH homologues). The formation of the 7,12-dihydroquinone structure present in both reaction products is generally thought to occur nonenzymatically (I, II).

These results suggest that the extracted red reaction intermediate would be 12-hydroxy-prejadomycin, which is used as a substrate by the monooxygenases when catalyzing 12b-hydroxylation (Figure 17). The hydroxylation of C-12 by the monooxygenases is very likely catalyzed according to the classical reaction mechanism for aromatic hydroxylases belonging to the family of FPMO (Figure 3) (Massey, 2000). However, the reaction mechanism utilized by the angucycline monooxygenases for the hydroxylation of position C-12b of 12-hydroxy-prejadomycin is uncertain. Recent activation experiments with *Streptomyces* sp. PGA64, which contains the silent *pga* gene cluster, showed that this cluster is capable of producing fridamycin-type metabolites. Based on this finding, the authors suggested that PgaE would act as Baeyer-Villiger monooxygenase and insert an oxygen atom between C-1 and C-12b of 12-hydroxy-prejadomycin, as suggested previously for UrdM in the biosynthesis of urdamycins (Guo et al, 2015, Rix et al., 2003). The Baeyer-Villiger oxygenation would be followed by a rearrangement reaction to produce 12b-hydroxylated product or dehydration to produce a fridamycin-type compound (Guo et al., 2015). However, in the absence of experimental proofs, neither of these reaction mechanisms for 12b-hydroxylation can be verified.

The production of 11-deoxylandomycinone from 12-hydroxy-prejadomycin can only be achieved by the simultaneous presence of one of the monooxygenases LanE, UrdE, PgaE or CabE and the SDR enzyme LanV in the absence of molecular oxygen,

indicating that the monooxygenases are required for a reaction other than hydroxylation (II). One of the most significant differences between the biosynthesis of gaudimycin C and 11-deoxylandomycinone is the stereochemistry of 6-ketoreduction (Figure 17). The stereochemistry of the C-6 hydroxyl group of 11-deoxylandomycinone is known to be *R* whereas the equivalent hydroxyl in gaudimycin C was assigned as *S* by comparison of the experimental and calculated ECD spectra (Figure S4 in II). This indicates that besides the different substrates for the ketoreduction, LanV and other 6-ketoreductases also have different stereospecificities in 6-ketoreductions (Figure 17) (II).

4.1.4 Hidden activities of the modifying enzymes

Experiments with different substrates, reaction conditions and enzyme combinations showed that all of the angucyclinone tailoring enzymes contain latent context-dependent catalytic activities. Both of the hydroxylations, C-12 and C-12b, are expected to take place in the urdamycin and gaudimycin pathways, but the 12b-hydroxyl group is absent in landomycins and jadomycins. Despite the absence of 12b-hydroxyl groups in their natural pathways, LanE and JadH are both capable of catalyzing the 12b-hydroxylation of 12-hydroxy-prejadomycin. In the case of LanE, this can be seen in a coupled reaction with LanE and CabV or UrdMred, which produces gaudimycin C from prejadomycin. In the case of JadH, 12b-hydroxylation activity can only be detected if extracted 12-hydroxy-prejadomycin is used as a substrate for a coupled reaction of JadH and any of the SDR enzymes as these reactions produce gaudimycin C (Figure 5 in II) (II).

In the case of 6-ketoreductases, the latent activities could be detected by using different substrates in the reactions. The coupled reactions of the monooxygenases LanE, UrdE, PgaE or CabE and the ketoreductases CabV or UrdMred produced 11-deoxylandomycinone from 12-hydroxy-prejadomycin when the hydroxylation activity of the monooxygenases was inhibited by removing molecular oxygen from the reaction mixture (Figure S5 in II). In the presence of molecular oxygen, the monooxygenases and LanV can catalyze the conversion of 12-hydroxy-prejadomycin into gaudimycin C. These results demonstrate that all the ketoreductases in this study are able to catalyze ketoreductions with both 6*R* and 6*S* stereochemistries (Figure 5 in II) (II).

The most drastic example of the context-dependent activities of the angucyclinone tailoring enzymes can be seen in the formation of gaudimycin C from 12-hydroxy-prejadomycin by JadH and LanV. In this reaction, both of the enzymes catalyze reactions unnecessary in their natural pathways: 12b-hydroxylation by JadH and ketoreduction with 6*S* stereochemistry by LanV (Figure 5 in II) (II).

4.2 Mutagenesis studies of PgaE (original publication III)

The analysis of the crystal structures of PgaE and CabE (Koskiniemi et al. 2007) and the structure-based sequence alignment of PgaE, LanE, CabE, UrdE, JadH, GilOI (gilvocarcin pathway) (Fischer et al., 2003), and AlpG (kinamycin pathway) (Pang et al., 2004) revealed four distinct regions that were different around the active site cavities of enzymes catalyzing two consecutive hydroxylations (PgaE, LanE, CabE, and UrdE) and enzymes catalyzing 12-hydroxylation together with 4a,12b-dehydration (JadH, AlpG, and GilOI) (Figure 18 and Figure S3 in III). The GilOI and AlpG are FPMOs orthologous to JadH, which have been shown to be involved in the conversion of prejadomycin into dehydrorabelomycin by *in vitro* experiments (Pahari et al., 2012) and phylogenetic analysis (Palmu et al. 2007), respectively. The four regions were targeted with mutagenesis experiments where regions of PgaE were replaced with JadH sequences using a modified four-primer overhang extension PCR method (see section 3.1).

4.2.1 Effect of the different mutagenesis regions

The spectrophotometric analysis of different PgaE variant reactions revealed several different chimeric enzymes where the activity differed from the native PgaE. The β4–β5 region (residues 70–82 of PgaE) was found to have a dramatic effect on the 12b-hydroxylation activity of PgaE; while the 12-hydroxylation activity of the PgaE β4–β5 variant was comparable to native PgaE, the 12b-hydroxylation activity was significantly lowered (Figure 3 in III). After this finding, we decided to test the effect of three additional regions, β6 (residues 92–94), β14 (residues 189 and 190), and β15–β16 (residues 201–209), in combination with the β4–β5 region on the activity of PgaE (III).

The change of regions β6 or β15–β16 together with region β4–β5 had no additional effect on the activity of PgaE, but the PgaE variant β4–β5/β14 surprisingly showed 12b-hydroxylation activity close to the native PgaE. The change of the β6 region in addition to regions β4–β5 and β14 further increased the 12b-hydroxylation activity of the enzyme variant. Both other triple variants, as well as the quadruple variant, showed 12b-hydroxylation activity similar to the PgaE β4–β5. Despite the fact that, various mutagenesis regions had an effect on the 12b-hydroxylation activity, all different PgaE variants were able to catalyze the 12-hydroxylation reaction. This is expected, because JadH, which was used as a template, also catalyzes the hydroxylation of the C-12 position of prejadomycin. These results show that, although the β4–β5 region is clearly important for the 12b-hydroxylation activity of PgaE, other regions around the active site cavity can also have an effect on the activity of the enzyme (Figure 3 in III) (III).

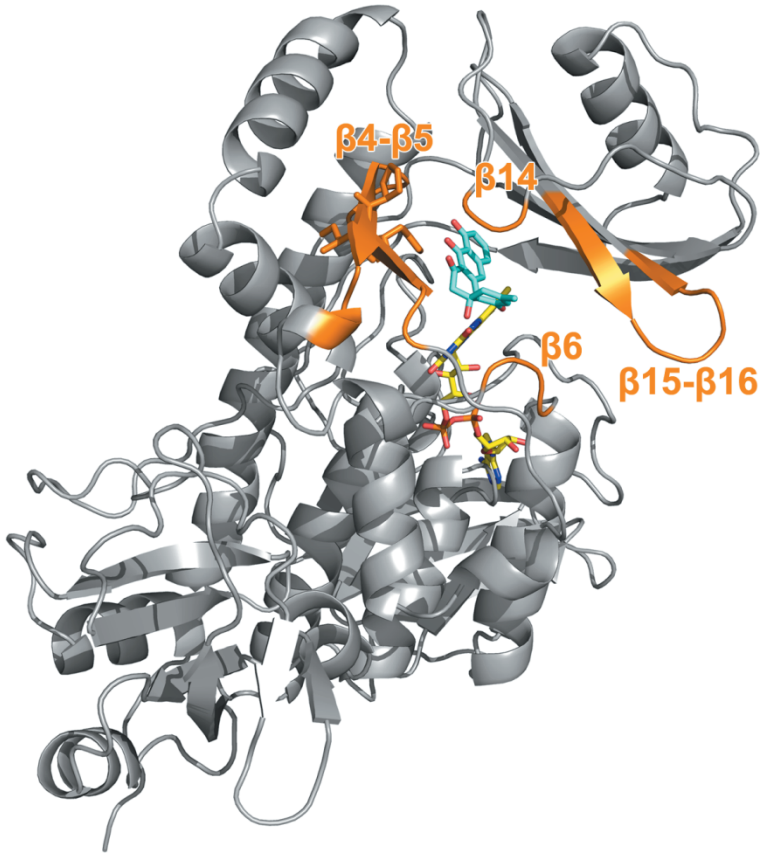

Figure 18: The crystal structure of PgaE in complex with FAD (shown in yellow) (PDB code 2QA1). The four mutagenesis regions around the active site cavity of PgaE are shown in orange and labeled as β4–β5, β6, β14 and β15–β16. The amino acid residues His-73, Pro-78 and Ile-79 discussed below are shown as sticks within the β4–β5 region. The substrate prejadomycin shown in cyan was docked into the active site.

4.2.2 Dissection of the β4–β5 region

As the β4–β5 area was found to be the most significant region in changing the activity of PgaE, this region was dissected to smaller subregions in order to find out the exact amino acids behind the changes. The region was first divided into two halves: strands β4 (amino acids 70–71) and β5 (77–82). The kinetic analysis of these variants clearly showed that the change of β4 had no effect on the PgaE activity whereas the PgaE β5 variant displayed dramatically decreased 12b-hydroxylation activity and lowered substrate inhibition (Figures S2 and S5 in III) (III).

Further dissection of the β5 region by changing Pro-78 and Ile-79 to the corresponding JadH amino acids glutamine and phenylalanine, respectively, revealed an interesting correlation between these residues and 12b-hydroxylation activity. The PgaE variant P78Q showed about 2.5-fold increase in the efficiency of 12b-hydroxylation (k_{cat}/S_{50}

of 7.76 x 10^5 $M^{-1}s^{-1}$ vs. 2.99 x 10^5 $M^{-1}s^{-1}$) compared to the native PgaE whereas the change I79F generated a variant with only 14% of the 12b-hydroxylation activity left (k_{cat}/S_{50} 4.09 x 10^4 $M^{-1}s^{-1}$). The PgaE double variant P78Q/I79F also showed significantly lower 12b-hydroxylation activity than the native PgaE (k_{cat}/S_{50} 2.34 x 10^4 $M^{-1}s^{-1}$), but the substrate inhibition in 12-hydroxylation was comparable to the effect seen in the native enzyme (III).

The data acquired from spectrophotometric measurements with substrates prejadomycin and 12-hydroxy-prejadomycin were analyzed by fitting the data into various kinetic models which all indicated the presence of two substrate binding sites in one monomer of PgaE. Despite the considerable flexibility in the parameter values, all of the models used indicated that there was a clear correlation between the relaxation of substrate inhibition and the decreased 12b-hydroxylation activity. The results were, in most cases, inadequate to distinguish whether the alleviated substrate inhibition was due to changes in (i) the substrate affinity, (ii) the ratio of bisubstrate and monosubstrate complex activities or (iii) the ratio of the bisubstrate and monosubstrate complex dissociation constants (see section 3.5 and Supplementary Text of III) (III).

4.2.3 Effect of a conserved histidine on the 12b-hydroxylation activity

One histidine residue (His-73 in PgaE) residing in the β4 sheet close to amino acids Pro-78 and Ile-79 is conserved in all known angucyclinone hydroxylases (Figure S3 in III). The role of this histidine as a potential catalytic base has been studied previously, and it was shown that the change of this residue to alanine has no effect on the 12-hydroxylation activity of PgaE (Koskiniemi et al., 2007). Our kinetic analysis revealed the fact that, while the PgaE H73A variant was able to catalyze the hydroxylation of prejadomycin at C-12, the 12b-hydroxylation activity of this variant was completely abolished and 12-hydroxy-prejadomycin was detected as the reaction product. Also, no substrate inhibition effect was observed in the 12-hydroxylation reaction catalyzed by PgaE H73A variant; a fact that further highlights the correlation between 12b-hydroxylation activity and substrate inhibition in 12-hydroxylation. The kinetic model used to fit the data from the measurements with PgaE H73A contained only one independent binding site and needed no cooperativity between the monomers (III).

4.2.4 Model for the hydroxylation activities of PgaE

Based on the kinetic analysis of the different PgaE variants and the structural information from the PgaE P78Q/I79F crystal structure, we were able to propose a model for the PgaE activity that would explain all of the unusual features of this enzyme: bifunctionality, temporal separation of 12- and 12b-hydroxylation and the substrate inhibition affecting the hydroxylation of C-12 position but not C-12b (III).

Our model proposes that there are two overlapping binding sites in the active site of PgaE: one for prejadomycin and one for 12-hydroxy-prejadomycin. The maximum activity of 12-hydroxylation would be achieved when the prejadomycin binding site of only one monomer in the PgaE dimer is occupied. If prejadomycin is bound to the active sites of both monomers, lower enzymatic activity is observed due to allosteric effects caused by substrate binding. At the same time, prejadomycin is also able to bind to an overlapping binding site of 12-hydroxy-prejadomycin in a noncatalytic orientation. This binding also causes the same allosteric effects as the binding to the prejadomycin binding site and lowers the 12-hydroxylation activity of the other monomer. These features would explain the substrate inhibition effect observed in the 12-hydroxylation catalyzed by PgaE and the temporal separation of these two reaction phases, if the binding of prejadomycin to other monomer would prevent the binding of 12-hydroxy-prejadomycin to the other monomer as well (Figure 4 in III) (III).

In this model, 12-hydroxy-prejadomycin is able to bind only to the binding site intended for it, and the maximum activity is observed when binding sites of both monomers are occupied. The binding of 12-hydroxy-prejadomycin induces allosteric effects, which can be seen as a sigmoidal relationship in the kinetic data. Cooperative binding caused by the allosteric effects can further enhance the temporal separation of the 12- and 12b-hydroxylations as the 12b-hydroxylation activity is mainly derived from the bisubstrate complex, which is formed only under high concentrations of 12-hydroxy-prejadomycin (Figure 4 in III) (III).

The structure of the PgaE P78Q/I79F variant (PDB code 4ICY) showed that the mutated amino acids are actually pointing away from the active site toward the α13 helix involved in the formation of the dimer interface. The His-73 residue, which points toward the active site cavity of PgaE, is most likely involved in the binding of angucycline substrates to the binding site intended for 12b-hydroxylation, as both 12b-hydroxylation activity and substrate inhibition in 12-hydroxylation reaction are completely inhibited in the PgaE H73A variant. The fact that residues His-73, Pro-78 and Ile-79 are all affecting both substrate inhibition and 12b-hydroxylation led us to speculate that these residues are involved in the formation of a network behind the allosteric effects. The His-73 residue would be important for the formation of the allosteric effects whereas residues Pro-78 and Ile-79 would be required for the communication between the two subunits of the PgaE dimer (Figure 1 in III) (III).

4.3 Structures of LanV and UrdMred (original publications IV–V)

Crystal structures of LanV in complex with $NADP^+$, $NADP^+$ + 11-deoxylandomycinone and $NADP^+$ + rabelomycin and UrdMred in complex with $NADP^+$ + rabelomycin were determined at 1.65 Å, 2.0 Å, 2.50 Å and 2.25 Å resolution, respectively. The structures revealed that these two enzymes are highly similar in structure and contain all the features typical for enzymes belonging to the SDR superfamily (IV, V).

4.3.1 Overall structures of and differences between LanV and UrdMred

The overall structures of LanV and UrdMred both consist of a central seven-stranded parallel β-sheet surrounded by three parallel α-helices on each side, which is a classical Rossmann fold (Figure 2 in V). The characteristic N-terminal TGXXXGXG motif involved in the dinucleotide binding is also found in both enzymes (Figure 3 in V). Altogether the structures of LanV and UrdMred are very similar with the root-mean-square deviation (rmsd) of 1.18 Å between the $NADP^+$ + rabelomycin complex structures of these enzymes. The binding of the substrate in both enzymes takes place mainly through hydrophobic interactions with the amino acid residues around the substrate binding cavity (Figure 3 in IV, Figure 2 in V) (IV, V).

The biggest differences between LanV and UrdMred are found around the active site cavity. LanV binds the 2'-phosphate of $NADP^+$ with the backbone amide groups of Ala-38–Gly-40 while Arg-16 participates in the coordination from the opposite side of Ala-38 (Figure 3 in IV). In UrdMred, a more bulky Ser-38 causes such a shift in the corresponding loop region that only the backbone amides of Ser-38 and Arg-16 are involved in the coordination of the 2'-phosphate of $NADP^+$. These results suggest that UrdMred is less optimized for NADPH binding than LanV. The second difference between these enzymes is the shape of the active site cavity; in UrdMred, the active site is in a more open conformation than in LanV resulting in a larger active site volume (Figures 2 and S2 in V). Another difference is found in the binding of the ligand rabelomycin. The planar anthraquinone part of the rabelomycin is tilted by 9° toward Leu-149 in UrdMred compared to LanV (Figure 2D in V). This tilt is partially caused by changes in the length of the side chain of residues Ser-192 and Ile-192 in LanV and UrdMred, respectively. The bulkier side chain of Ile-192 pushes the planar anthraquinone toward Leu-149 in UrdMred, causing the observed tilt in the position of rabelomycin (IV, V).

In the complex structure of LanV and $NADP^+$ + 11-deoxylandomycinone, the ketoreduction has proceeded to reverse direction in the crystal as the electron density of the ligand fit best with 6-keto form of 11-deoxylandomycinone. This complex structure also shows a coordinated water molecule between Tyr-160 and the C-6-keto group of the ligand (Figure 3D in IV). This water molecule is not present in LanV and UrdMred complex structures with $NADP^+$ + rabelomycin (IV,V).

4.3.2 Comparison of LanV and UrdMred to other ketoreductases

The overall structures of most of the SDR enzymes involved in the biosynthesis of natural products are very close to the structures of LanV and UrdMred, as the Rossmann fold is one of the main features in the members of this enzyme superfamily. Major differences can be observed when LanV and UrdMred are compared to the enzymes involved in sugar biosynthesis. These enzymes belong to a group of extended SDR enzymes, which have an additional ~100 residue C-terminal domain compared to classical SDR enzymes

like LanV and UrdMred (Kavanagh et al., 2008). These C-terminal domains are involved in the correct positioning of the NDP-sugars (Allard et al., 2001a)

When comparing LanV and UrdMred with their closest homologues involved in natural product biosynthesis, the biggest differences are found in the α7 region. This flap-like structure is 11 amino acids longer in related polyketide reductases ActKR (Hadfield et al., 2004, Korman et al., 2004) and HedKR (Javidpour et al., 2011) (Figure 2 in IV), which are involved in the biosynthesis of actinorhodins and hedamycins, respectively. These longer "lid" helices form an additional helix, which has been suggested to open and close the active site entrance during the catalytic cycle (Hadfield et al., 2004, Javidpour et al., 2011, IV, V).

4.3.3 Proposed mechanism for the activity of LanV

The catalytic mechanism of 6-ketoreduction catalyzed by LanV is very similar to other well studied classical SDR enzymes (Filling et al., 2002, Oppermann et al., 2003). Based on the sequence and structure of LanV in complex with $NADP^+$ and the 6-keto form of 11-deoxylandomycinone, all the amino acids of the catalytic tetrad, Asn-121, Ser-147, Tyr-160, and Lys-164, are present in the active site cavity (Figure 3 in IV). The coordinated water molecule found between Tyr-160 and the 6-keto group of the ligand may be involved in the proton transfer from tyrosine to the substrate. The Ser-147 also forms a hydrogen bond with the coordinated water molecule, and it is thus unlikely that this residue is involved in substrate polarization as suggested in the other SDR enzymes (Filling et al., 2002). The Asn-121 residue in LanV corresponds to Asn-111 in 3β/17β-hydroxysteroid dehydrogenase, which has been shown to coordinate with a water molecule involved in the proton relay system of this SDR enzyme (Filling et al., 2002). In the case of LanV, Asn-121 cannot be involved in this function as there are no coordinated water molecules present in the vicinity of the side chain carbonyl group (IV).

The mutation of Tyr-160 to alanine resulted in the complete loss of LanV activity in a coupled reaction with the monooxygenases LanE, UrdE, PgaE or CabE, indicating that Tyr-160 is important for the proton transfer involved in 6-ketoreduction (Figure 4 in IV). The second phase of the 6-ketoreduction catalyzed by LanV is the hydride transfer from NADPH to the C-6 of the substrate. This was shown to take place from the 4-*pro*-S side of the NADPH by using stereospecifically labeled $NADP^2H$. The LC-MS-analysis of the 11-deoxylandomycinone from the coupled reaction of PgaE and LanV using the deuterium-labeled NADPH showed an increase of mass by 0.99 Da, consistent with the incorporation of one deuterium atom (Figure 5 in IV). Together with the structural and sequence information on the active site of LanV, these results confirm that the catalysis of the 6-ketoreduction in LanV takes place through a mechanism common for the enzymes of the SDR superfamily with some minor differences as mentioned above (Figure 6 in IV) (IV).

4.4 Mutagenesis studies of LanV and CabV (original publication V)

The comparison of the crystal structures of LanV and UrdMred and the sequences of the orthologous SDR enzymes CabV and PgaMred revealed four regions around the active site cavities that differed between LanV and other angucyclinone 6-ketoreductases (Figures 17 and 19). These enzymes are all highly similar in amino acid sequences; in the case of LanV and CabV, the sequence identity is 68%. The idea of these mutagenesis studies was to interchange these four regions between LanV and CabV in all possible combinations in order to elucidate the regions of the active sites behind the different stereospecificities of these enzymes. Since the structures of the enzymes implicated that the overall hydrophobic shape of the active site instead of individual amino acids is the key to the substrate binding, the mutagenesis was carried out by changing large regions of the enzymes and not individual amino acids (V). Also, the mutagenesis studies with PgaE and JadH had given implications that the activity of the enzyme can be affected by several large regions on different positions around the active sites of the enzymes (III). The regions changed in this study were amino acids 102–118 (R1), 154–163 (R2), 192 (Ser in LanV, Ile in CabV, R3) and 198–210 (R4) (V).

4.4.1 Effect of the single mutagenesis regions

The R3 region was the only mutagenesis region that had a major effect on the activities of LanV and CabV alone, whereas all the other regions had only small effects on the functions of these enzymes. The native LanV produces only 11-deoxylandomycinone, while native CabV produces 11-deoxylandomycinone and gaudimycin C in a 1:11 ratio. The exchange of R3 changed the activities of LanV and CabV to produce 11-deoxylandomycinone and gaudimycin C in 3:2 and 2:3 ratios, respectively. The effect of R3 on the enzymatic activities can be partially explained by the structures of LanV and UrdMred in complex with $NADP^+$ and rabelomycin; the difference between the side chains of serine and isoleucine in LanV and UrdMred (also CabV), respectively, causes the planar anthraquinone of rabelomycin to tilt by nine degrees toward leucine 149. This difference can have an effect on the positioning of the substrates in LanV and CabV and change the stereochemical outcome of 6-ketoreduction.

4.4.2 Activities of the double, triple and quadruple variants

The importance of R3 was also highlighted in double variants of LanV and CabV, where LanV variants R2+R3 and R1+R3 and CabV variant R1+R3 had the largest effect on the stereochemistry of 6-ketoreduction. The regions R2+R3 in LanV and R1+R3 in CabV were important factors for the control of the stereochemistry also in LanV and CabV triple variants; both LanV variants R1+R2+R3 and R2+R3+R4 produce almost equal amounts of 11-deoxylandomycinone and gaudimycin C, and in the case of CabV, the R1+R3+R4 variant produces these products in a 7:1 ratio. With both enzymes, the largest effect on the stereochemistry of 6-ketoreduction was observed with the quadruple variants. The

quadruple variant of LanV produced 11-deoxylandomycinone and gaudimycin C in 1:4 ratio whereas the ratio of the products with CabV quadruple variant was 16:1 (Figure 4 in V) (V).

All of the generated enzyme variants, where the activity differed from the activity of the native enzyme, produced a mixture of 11-deoxylandomycinone and gaudimycin C in different ratios. There were no enzyme variants able to catalyze the formation of these products with reverse stereochemistries at C-6: 6*S*-11-deoxylandomycinone or 6*R*-gaudimycin C, which is a known compound called gaudimycin B (Figure S3 in V) (Palmu et al., 2007). These results indicate that the stereospecificity of the ketoreduction is strongly related to the substrate specificity of the enzyme (V).

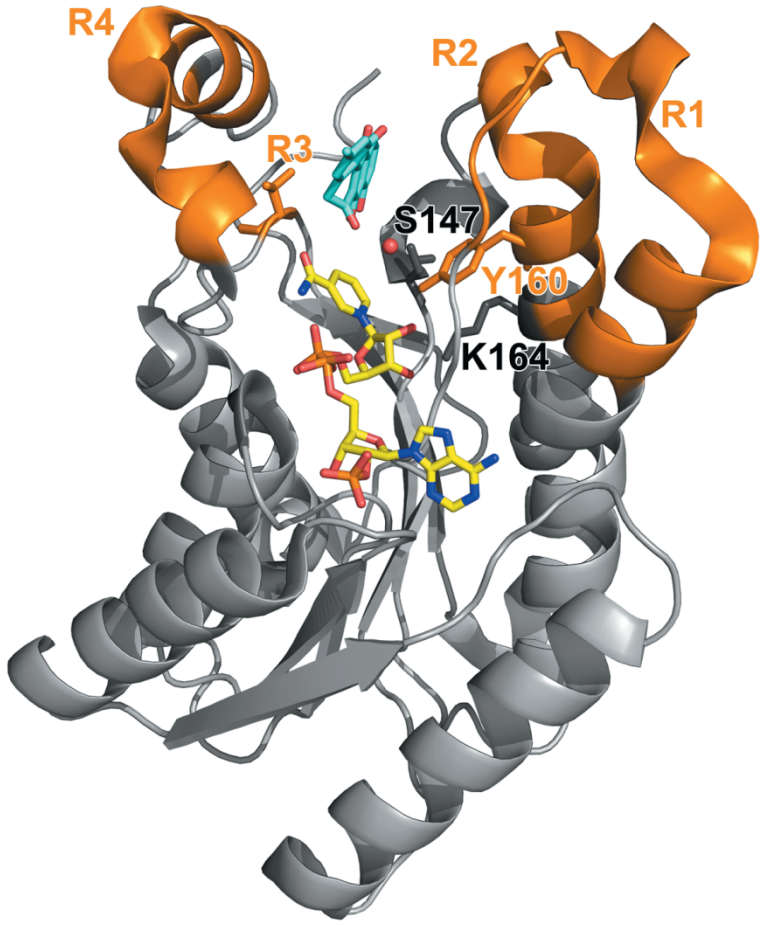

Figure 19: The structure of LanV in complex with $NADP^+$ and 11-deoxylandomycinone (PDB code 4KWI). The mutagenesis regions around the active site of LanV are shown in orange, 11-deoxylandomycinone in cyan and $NADP^+$ in yellow. The catalytic amino acid residues Ser-147 (dark grey), Tyr-160 (orange) and Lys-164 (dark grey) are shown as sticks and the coordinated water molecule between Tyr-160 and 11-deoxylandomycinone as a red sphere.

4.4.3 Factors behind the different stereochemistries of angucyclinone 6-ketoreductions

The docking studies performed with LanV and UrdMred and their products 11-deoxylandomycinone and gaudimycin C, respectively, further highlighted the inherent relationship between the substrate specificity of the angucyclinone 6-ketoreductases and the stereochemical outcome of these reactions. With both enzymes, the stereochemical outcome of the reaction could be explained based on the docking results. In the case of LanV, it seemed that the coordinated water molecule present in the crystal structure of LanV in complex with $NADP^+$ and 11-deoxylandomycinone was required for the relay of a proton from Tyr-160 to the C-6 carbonyl oxygen in the formation of the 6*R* stereochemistry (Figure 5 in V). The docking experiments with the unnatural products of LanV and UrdMred, gaudimycin C and 11-deoxylandomycinone, respectively, also showed the correct positioning of the catalytic amino acids, 4-*pro*-S hydride of the NADPH and the C-6 of the ligand for the formation of the C-6 stereochemistry observed in these metabolites (Figure S5 in V) (V). This is in agreement with the findings that both of these enzymes, as well as CabV, are able to catalyze the formation of both 6*R* and 6*S* stereochemistry depending on whether the product of the reaction is 11-deoxylandomycinone or gaudimycin C (see section 4.1.4) (II).

As a consequence of these findings, it seems probable that in order to change the stereochemistries of these angucycline 6-ketoreductases, amino acids not found in native LanV or CabV would have to be introduced to the active sites of these enzymes. Since the change in stereochemistry of the reaction is dependent on the conformation of the substrate, the overall shape of the active site has to be changed in order to create angucyclines with altered stereochemistries at C-6 hydroxyl groups. These mutations would have to change the shape of the active site to position the 6-keto groups of the potential substrates in opposite orientation between the catalytic tyrosine and 4-*pro*-S hydride of the NADPH.

4.5 Evolution of the different pathways (original publications I–III, V)

The different reaction cascades that convert prejadomycin to three alternative products, dehydrorabelomycin, gaudimycin C and 11-deoxylandomycinone, gave insights into the evolution of the different angucycline pathways (Figure 17). The results of the coupled reactions with the monooxygenases and the reductases implicated that the outcome of these reactions depends solely on the SDR component present in the reaction mixture. In the presence of the monooxygenase and LanV, 11-deoxylandomycinone is formed while replacement of LanV with the other reductase components, CabV, UrdMred or PgaM, yields gaudimycin C. These findings indicated that the origin of the landomycin pathways was the evolution of LanV to act before the 12b-hydroxylation has taken place (I, II).

The mutagenesis studies with LanV and CabV revealed that the stereochemical outcome of the ketoreductions catalyzed by these enzymes depends mostly on the conformation of the substrate used by the enzyme. The modeled structures of 11-deoxylandomycinone, gaudimycin C and other angucyclinones from the pathways involved in this study showed that 4a,12b-dehydration causes significant changes to the conformation of these metabolites (Figure S4 in V). The evolution of landomycins from other angucyclines can therefore be explained by the gained ability of LanV to catalyze 6-ketoreduction to the substrate which has gone through 4a,12b-dehydration. Whether this dehydration is catalyzed by LanE or LanV and how the 12b-hydroxylation reaction by LanE is inhibited remains elusive, since these steps cannot be separated from each other (V).

The different activity of JadH compared to the other monooxygenases in this study indicates that JadH is the key enzyme that differentiates the jadomycin pathway from the urdamycin, landomycin and gaudimycin pathways. The ability of JadH to convert prejadomycin to dehydrorabelomycin by catalyzing 12-hydroxylation and 4a,12b-dehydration without the release of the intermediate product steers the biosynthesis toward jadomycins. The evolution behind this has been the change of the second catalytic activity of JadH from 12b-hydroxylation to 4a,12b-dehydration. This change may be a consequence of the increased affinity of JadH towards 12-hydroxy-prejadomycin, which prevents the dissociation of 12-hydroxy-prejadomycin after the first reaction and makes the catalysis of 4a,12b-dehydration possible (II, III).

The mutagenesis experiments with PgaE revealed that the active site of PgaE is surprisingly flexible, and there are several possible scenarios to how the change of activities between PgaE and JadH could have occurred (Figure 3 in III). The minimum change to inhibit the 12b-hydroxylation activity in JadH has been the change of amino acids Pro-78 and Ile-79 to glutamine and phenylalanine, respectively. At the level of DNA, this requires a change of two nucleotides, c*cga*tc to c*agt*tc. After the inhibition of the 12b-hydroxylation activity, JadH has improved its 4a,12b-dehdyration activity to produce dehydrorabelomycin. The exact changes that have occurred in the evolution of JadH to enable the production of jadomycins are not clear, since changing all the different amino acids around the active site of PgaE was not enough to generate a dehydrorabelomycin producing enzyme. However, the studies show that after the changes in the β4–β5 region, the changes in other regions could have taken place without affecting the ability of the enzyme to catalyze 12-hydroxylation and without restoring the 12b-hydroxylation activity (III).

5. CONCLUDING REMARKS

In this study, it was shown that tailoring enzymes from different angucycline pathways can catalyze the conversion of a common intermediate, prejadomycin, into three different products, dehydrorabelomycin, 11-deoxylandomycinone and gaudimycin C. Dehydrorabelomycin and 11-deoxylandomycinone have been shown to be intermediates in the biosynthetic pathways of jadomycins and landomycins, respectively. This study also showed that all flavoprotein monooxygenases involved in these reactions are able to catalyze both 12- and 12b-hydroxylations as well as the 4a,12b-dehydration reaction. Also, the short-chain alcohol dehydrogenase/reductaces from these reaction cascades were shown to contain the ability to catalyze 6-ketoreduction with both possible stereospecificities.

The clarification of the tailoring reactions taking place during the biosynthesis of different angucyclines revealed that the enzymes JadH and LanV present the branching points of the jadomycin and landomycin pathways, respectively, from the urdamycin and gaudimycin pathways. A closer analysis of these reactions by mutagenesis experiments revealed differences between homologous enzymes that are behind the different activities.

The kinetic analysis of native PgaE and several variant enzymes revealed a correlation between the substrate inhibition in 12-hydroxylation and the ability to catalyze 12b-hydroxylation. It seems that the substrate inhibition in PgaE is a consequence of the ability of the enzyme to catalyze two consecutive hydroxylations in the same active site. The analysis of the differences between LanV and CabV revealed that the different stereospecificities of these enzymes are actually due to the different conformations of their substrates.

The results also showed that, even after the differentiation of the biosynthetic pathways to produce distinct metabolites, these enzymes still possess the ability to catalyze reactions, which are no longer required in their pathways. Also, enzymes from the *urd*, *pga* and *cab* pathways have the ability to catalyze reactions, which are not required in the biosynthesis of urdamycins and gaudimycins, but have evolved as the main functions for JadH and LanV. In the case of JadH, the mutations that have weakened the ability of the enzyme to catalyze the 12b-hydroxylation, have enabled the evolution of the 4a,12b-dehydration into a primary function. However, in the case of LanV, the enzyme has gained affinity toward an earlier pathway intermediate, but simultaneously, the greatly different conformation of the substrate has forced the enzyme to change its stereospecificity.

These enzymes with latent context-dependent activities are excellent examples of how promiscuity is used to aid the enzyme evolution. The promiscuous activities of the enzymes are thought to serve as a starting point for the generation of novel functions. The emergence of new enzyme activities occurs most likely gradually through active “intermediate” enzymes (Khersonsky and Tawfik, 2010). This phenomenon is also seen

in the mutagenesis experiments conducted with enzyme pairs PgaE/JadH and LanV/CabV. Especially in the case of LanV and CabV, several intermediate variants can be seen before the hidden activity evolves into the primary activity of the enzyme.

One current model for enzyme evolution is the escape from adaptive conflict (EAC). In this model, two activities of one enzyme cannot specialize simultaneously, but the enzyme remains bi-functional. These two activities can only evolve to primary functions after gene duplication event (Conant and Wolfe, 2008). The EAC model is especially well suited for the case of PgaE and JadH. In both enzymes, either 12b-hydroxylation or 4a,12b-dehydration has evolved to primary function while the other is still present as a secondary activity. This suggests that these enzymes have not yet become specialized but are still evolving. However, it is uncertain to what extend is this kind of specialization necessary for enzymes involved in the biosynthesis of secondary metabolites, as the promiscuity enables rapid evolution of new enzyme activities – a trait useful in the generation of new secondary metabolites.

ACKNOWLEDGEMENTS

The experimental laboratory work related to this thesis was conducted over the years 2010–2014 at the Department of Biochemistry (former Department of Biochemistry and Food Chemistry) in the Antibiotic Biosynthetic Enzymes (ABE) research group. The work was financially supported by the Academy of Finland, the Finnish Cultural Foundation, National Doctoral Programme in Informational and Structural Biology (ISB) and the University of Turku Graduate School (UTUGS). The interesting conference trips during the thesis work were funded by the ISB, Turku University Foundation and Turku Centre for Systems Biology. I want to thank professors Jyrki Heino and Reijo Lahti for providing the inspirational and fun working environment at Arcanum.

I want to thank the reviewers of my thesis, Doreen Dobritzsch and Lari Lehtiö, for constructive criticism and comments to improve the quality of this thesis. I also want to thank my ISB Thesis Committee member Jussi Meriluoto for his comments during my thesis work.

A big thank you belongs to my supervisors, Mikko Metsä-Ketelä and Jarmo Niemi, for the support, ideas and advice during this thesis work. It has been extremely interesting and educational to work with this diverse project and in this research group.

I also want to thank all the other people who have been involved in this project: our collaborators, Prof. Keqian Yang from the Chinese Academy of Sciences, Prof. Jürgen Rohr from the University of Kentucky, Karel Klika, Petri Tähtinen, Jukka-Pekka Suomela and Georgiy Belogurov from the University of Turku, as well as present and former members of the ABE research group, Prof. Emeritus Pekka Mäntsälä, Laila Niiranen, Keshav Thapa and Pasi Paananen. I owe an especially big thank you to Pauli Kallio who introduced me to the fascinating world of angucycline tailoring enzymes and has supported me during our work together.

It has been extremely nice to work in the ABE research group and I want to thank all the present and former members for creating this great atmosphere: Vilja, Terhi, Thadée, Bastian, Pedro, Nadine, Linnea and all the students who have been working with us during these years. I also want to thank all the personnel from the Biochemistry unit for the nice working environment.

I want to thank my whole family and other relatives for support and encouragement during my studies and thesis work. Especially big thank you belongs to Johanna and Aada for all the love, joy and support I have received during these years.

REFERENCES

Alfieri, A., Malito, E., Orru, R., Fraaije, M. W., and Mattevi, A. **(2008)** Revealing the Moonlighting Role of NADP in the Structure of a Flavin-Containing Monooxygenase. *Proc. Natl. Acad. Sci. USA* **105**, 6572–6577.

Allard, S. T. M, Giraud, M.-F., and Naismith, J. H. **(2001a)** Epimerases: Structure, Function and Mechanism. *Cell. Mol. Life Sci.* **58**, 1650–1665.

Allard, S. T. M, Giraud, M.-F., Whitfield, C., Graninger, M., Messner, P., and Naismith, J. H. **(2001b)** The Crystal Structure of dTDP-D-Glucose 4,6-Dehydratase (RmlB) from *Salmonella enterica* Serovar Typhimurium, the Second Enzyme in the dTDP-L-Rhamnose Pathway. *J. Mol. Biol.* **307**, 283–295.

Allard, S. T. M, Beis, K., Giraud, M.-F., Hegeman, A. D., Gross, J. W., Wilmouth, R. C., Whitfield, C., Graninger, M., Messner, P., Allen, A. G., Maskell, D. J., and Naismith, J. H. **(2002)** Toward a Structural Understanding of the Dehydratase Mechanism. *Structure* **10**, 81–92.

Allard, S. T. M., Cleland, W. W., and Holden, H. M. **(2004)** High Resolution X-ray Structure of dTDP-Glucose 4,6-Dehydratase from *Streptomyces venezuelae*. *J. Biol. Chem.* **279**, 2211–2220.

Bailly, C., Riou, J.-F., Colson, P., Houssier, C., Rodrigues-Pereira, E., and Prudhomme, M. **(1997)** DNA Cleavage by Topoisomerase I in the Presence of Indolocarbazole Derivatives of Rebeccamycin. *Biochemistry* **36**, 3917–3929.

Balibar, C. J., and Walsh, C. T. **(2006)** In Vitro Biosynthesis of Violacein from L-Tryptophan by the Enzymes VioA-E from *Chromobacterium* V*iolaceum*. *Biochemistry* **45**, 15444–15457.

Ballou, D. P., Entsch, B., and Cole, L. J. **(2005)** Dynamics Involved in Catalysis by Single-Component and Two-Component Flavin-Dependent Aromatic Hydroxylases. *Biochem. Bioph. Res. Commun.* **338**, 590–598.

Blankenfeldt, W., Kerr, I. D., Giraud, M.-F., McMiken, H. J., Leonard, G., Whitfield, C., Messner, P., Graninger, M., and Naismith, J. H. **(2002)** Variation on a Theme of SDR: dTDP-6-Deoxy-L-*lyxo*-4-Hexulose Reductase (RmlD) Shows a New Mg^{2+}-Dependent Dimerization Mode. *Structure* **10**, 773–786.

Bradford, M. M. **(1976)** A Rapid and Sensitive Method for the Quantitation of Microgram Quantities of Protein Utilizing the Principle of Protein-Dye Binding. *Anal. Biochem.* **72**, 248–254.

Brodersen, D. E., Clemons, Jr., W. M., Carter, A. P., Morgan-Warren, R. J., Wimberly, B. T., and Ramakrishnan, V. **(2000)** The Structural Basis for the Action of the Antibiotics Tetracycline, Pactamycin, and Hygromycin B on the 30S Ribosomal Subunit. *Cell* **103**, 1143–1154.

Buysschaert, G., Verstraete, K., Savvides, S. N., and Verqauwen, B. **(2013)** Structural and Biochemical Characterization of an Atypical Short-Chain Dehydrogenase/Reductase Reveals an Unusual Cofactor Preference. *FEBS J.* **280**, 1358–1370.

Caffrey, P. **(2003)** Conserved Amino Acid Residues Correlating With Ketoreductase Stereospecificity in Modular Polyketide Synthases. *ChemBioChem* **4**, 649–662.

Chen, Y. H., Wang, C. C., Greenwell, L., Rix, U., Hoffmeister, D., Vining, L. C., Rohr, J., and Yang, K. Q. **(2005)** Functional Analyses of Oxygenases in Jadomycin Biosynthesis and Identification of JadH as a Bifunctional Oxygenase/Dehydrase. *J. Biol. Chem.* **280**, 22508–22514.

Chen, Y., Fan, K., He, Y., Xu, X., Peng, Y., Yu, T., Jia, C., and Yang, K. **(2010)** Characterization of JadH as an FAD- and NAD(P)H-Dependent Bifunctional Hydroxylase/Dehydrase in Jadomycin Biosynthesis. *ChemBioChem* **11**, 1055–1060.

Conant, G. C., and Wolfe, K. H. **(2008)** Turning a Hobby into a Job: How Duplicated Genes Find New Functions. *Nat. Rev. Genet.* **12**, 938–950.

Crozier-Reabe, K., and Moran, G. R. **(2012)** Form Follows Function: Structural and Catalytic Variation in the Class A Flavoprotein Monooxygenases. *Int. J. Sci.* **13**, 15601–15639.

Darken, M. A., Berenson, H., Shirk, R. J., and Sjolander, N. O. **(1960)** Production of Tetracycline by Streptomyces aureofaciens in Synthetic Media. *App. Microbiol.* **8**, 46–51.

Decker, H., and Haag, S. **(1995)** Cloning and Characterization of a Polyketide Synthase Gene from Streptomyces fradiae Tü2717, Which Carries the Genes for Biosynthesis of the Angucycline Antibiotic Urdamycin A and a Gene Probably Involved in Its Oxygenation. *J. Bacteriol.* **177**, 6126–6136.

Dennington, R., Keith, T., and Millam, J. **(2009)** GaussView, Version 5.0.8. (Shawnee Mission, KS: Semichem Inc.).

Dutton, C. J., Banks, B. J., and Cooper, C. B. **(1995)** Polyether Ionophores. *Nat. Prod. Rep.* **12**, 165–181.

Enroth, C., Neujahr, H., Schneider, G. & Lindqvist, Y. **(1998)** The Crystal Structure of Phenol Hydroxylase in Complex with FAD and Phenol Provides Evidence for a Concerted Conformational Change in the Enzyme and its Cofactor During Catalysis. *Structure* **6**, 605–617.

Enroth, C. **(2003)** High-Resolution Structure of Phenol Hydroxylase and Correction of Sequence Errors. *Acta Crystallogr. D* **59**, 1597–1602.

Entsch, B., Ballou, D. P., and Massey, V. **(1976)** Flavin-Oxygen Derivatives Involved in Hydroxylation by *p*-Hydroxybenzoate Hydroxylase. *J. Biol. Chem.* **251**, 2550–2563.

Entsch, B., and van Berkel, W. J. **(1995)** Structure and mechanism of para-hydroxybenzoate hydroxylase. *FASEB J.* **9**, 476–483.

Fabian, J. **(1965)** Simple Method of Anaerobic Cultivation, with Removal of Oxygen by a Buffered Glucose Oxidase-Catalase System. *J. Bacteriol.* **89**, 921.

Faust, B., Hoffmeister, D., Weitnauer, G., Westrich, L., Haag, S., Schneider, P., Decker, H., Künzel, E., Rohr, J., and Bechthold, A. **(2000)** Two New Tailoring Enzymes, a Glycosyltransferase and an Oxygenase, Involved in Biosynthesis of the Angucycline Antibiotic Urdamycin A in Streptomyces fradiae Tü2717. *Microbiology* **146**, 147–154.

Field, R. A., and Naismith, J. H. **(2003)** Structural and Mechanistic Basis of Bacterial Sugar Nucleotide-Modifying Enzymes. *Biochemistry* **42**, 7637–7647.

Filling, C., Berndt, K. D., Benach, J., Knapp, S., Prozorovski, T., Nordling, E., Ladenstein, R., Jörnvall, H., and Oppermann, U. **(2002)** Critical Residues for Structure and Catalysis in Short-chain Dehydrogenases/Reductases. *J. Biol. Chem.* **277**, 25677–25684.

Finlay, A. C., Hobby, G. L., P'an, S. Y., Regna, P. P., Routien, J. B., Seeley, D. B., Shull, G. M., Sobin, B. A., Solomons, I. A., Vinson, J. W., and Kane, J. H. **(1950)** Terramycin, a New Antibiotic. *Science* **111**, 85.

Fischer, C., Lipata, F., and Rohr, J. **(2003)** The Complete Gene Cluster of the Antitumor Agent Gilvocarcin V and its Implication for the Biosynthesis of the Gilvocarcins. *J. Am. Chem. Soc.* **125**, 7818–7819.

Frey, P. A., and Hegeman, A. D. **(2013)** Chemical and Stereochemical Actions of UDP-Galactose 4-Epimerase. *Acc. Chem. Res.* **46**, 1417–1426.

Frisch, M. J., Trucks, G. W., Schlegel, H. B., Scuseria, G. E., Robb, M. A., Cheeseman, J. R., Scalmani, G., Barone, V., Mennucci, B., Petersson, G. A., Nakatsuji, H., Caricato, M., Li, X., Hratchian, H. P., Izmaylov, A. F., Bloino, J., Zheng, G., Sonnenberg, J. L., Hada, M., Ehara, M., Toyota, K., Fukuda, R., Hasegawa, J., Ishida, M., Nakajima, T., Honda, Y., Kitao, O., Nakai, H., Vreven, T., Montgomery, J. A., Jr., Peralta, J. E., Ogliaro, F., Bearpark, M., Heyd, J. J., Brothers, E., Kudin, K. N., Staroverov, V. N., Kobayashi, R., Normand, J., Raghavachari, K., Rendell, A., Burant, J. C., Iyengar, S. S., Tomasi, J., Cossi, M., Rega, N., Millam, M. J., Klene, M., Knox, J. E., Cross, J. B., Bakken, V., Adamo, C., Jaramillo, J., Gomperts, R., Stratmann, R. E., Yazyev, O., Austin, A. J., Cammi, R., Pomelli, C., Ochterski, J. W., Martin, R. L., Morokuma, K., Zakrzewski, V. G., Voth, G. A., Salvador, P., Dannenberg, J. J., Dapprich, S., Daniels, A. D., Farkas, Ö., Foresman, J. B., Ortiz, J. V., Cioslowski, J., Fox, D. J. Gaussian09, Revision A.01 **(2009)** or Revision C.01 **(2010)** (Wallingford, CT: Gaussian, Inc.).

Garg, A., Xie, X., Keatinge-Clay, A., Khosla, C., and Cane, D. E. **(2014)** Elucidation of the Cryptic Epimerase Activity of Redox-Inactive Ketoreductase Domains from Modular Polyketide Synthases by Tandem Equilibrium Isotope Exchange. *J. Am. Chem. Soc.* **136**, 10190–10193.

Giessen, T. W., Kraas, F. I., and Marahiel, M. A. **(2011)** A Four-Enzyme Pathway for 3,5-Dihydroxy-4-methylanthranilic Acid Formation and Incorporation into the Antitumor Antibiotic Sibiromycin. *Biochemistry* **50**, 5680–5692.

Glaser, L. **(1963)** Biosynthesis of Deoxysugars. *Physiol. Rev.* **43**, 215–242.

Goldman, P. J., Ryan, K. S., Hamill, M. J., Howard-Jones, A. R., Walsh, C. T., Elliott, S. J., and Drennan, C. L. **(2012)** An Unusual Role for a Mobile Flavin in StaC-like Indolocarbazole Biosynthetic Enzymes. *Chem. Biol.* **19**, 855–865.

Graninger, M., Nidetzky, B., Heinrichs, D. E., Whitfield, C., and Messner, P. **(1999)** Characterization of dTDP-4-dehydrorhamnose 3,5-Epimerase and dTDP-4-dehydrorhamnose Reductase, Required for dTDP-L-rhamnose Biosynthesis in *Salmonella enterica* Serovar Typhimurium LT2. *J. Biol. Chem.* **274**, 25069–25077.

Guo, F., Xiang, S., Li, L., Wang, B., Rajasärkkä, J., Gröndahl-Yli-Hannuksela, K., Ai, G., Metsä-Ketelä, M., and Yang, K. **(2015)** Targeted Activation of Silent Natural Product Biosynthesis Pathways by Reporter-Guided Mutant Selection. *Metab. Eng.* **28**, 134–142.

Hadfield, A. T., Limpkin, C., Teartasin, W., Simpson, T. J., Crosby, J., and Crump, M. P. **(2004)** The Crystal Structure of the ActIII Actinorhodin Polyketide Reductase: Proposed Mechanism for ACP and Polyketide Binding. *Structure* **12**, 1865−1875.

Han, L., Yang, K., Ramalingam, E., Mosher, R. E., and Vining, L. C. **(1994)** Cloning and Characterization of Polyketide Synthase Genes for Jadomycin B Biosynthesis in *Streptomyces venezuelae* ISP5230. *Microbiology* **140**, 3379–3389.

Hertweck, C., Luzhetskyy, A., Rebets, Y., and Bechthold, A. **(2007)** Type II Polyketide Synthases: Gaining a Deeper Insight into Enzymatic Teamwork. *Nat. Prod. Rep.* **24**, 162–190.

Hertweck, C. **(2009)** The Biosynthetic Logic of Polyketide Diversity. *Angew. Chem. Int. Ed.* **48**, 4688–4716.

Ho, S. N., Hunt, H. D., Horton, R. M., Pullen, J. K., and Pease, L. R. **(1989)** Site-Directed Mutagenesis by Overlap Extension Using the Polymerase Chain Reaction. *Gene* **77**, 51−59.

Hotta, K., Chen, X., Paton, R. S., Minami, A., Li, H., Swaminathan, K., Mathews, I. I., Watanabe, K., Oikawa, H., Houk, K. N., and Kim, C.-Y. **(2012)** Enzymatic catalysis of anti-Baldwin ring closure in polyether biosynthesis. *Nature* **483**, 355–358.

Howard-Jones, A. R., and Walsh, C. T. **(2006)** Staurosporine and Rebeccamycin Aglycones Are Assembled by the Oxidative Action of StaP, StaC, and RebC on Chromopyrrolic Acid. *J. Am. Chem. Soc.* **128**, 12289–12298.

Huijbers, M. M., Montersino, S., Westphal, A. H., Tischler, D., and van Berkel, W. J. **(2014)** Flavin Dependent Monooxygenases. *Arch. Biochem. Biophys.* **544**, 2–17.

Husain, M., and Massey, V. **(1979)** Kinetic Studies on the Reaction of *p*-Hydroxybenzoate Hydroxylase. Agreement of Steady State and Rapid Reaction Data. *J. Biol. Chem.* **254**, 6657–6666.

Ichinose, K., Surti, C., Taguchi, T., Malpartida, F., Booker-Milburn, K. I., Stephenson, G. R., Ebizuka, Y., and Hopwood, D. A. **(1999)** Proof that the *Act*VI Genetic Region of *Streptomyces coelicolor* A3(2) Is Involved in Stereospecific Pyran Ring Formation in the Biosynthesis of Actinorhodin. *Bioorg. Med. Chem. Lett.* **9**, 395–400.

Javidpour, P., Das, A., Khosla, C., and Tsai, S. C. **(2011)** Structural and Biochemical Studies of the Hedamycin Type II Polyketide Ketoreductase (HedKR): Molecular Basis of Stereo- and Regiospecificities. *Biochemistry* **50**, 7426−7439.

Jones, G., Willett, P., Glen, R. C., Leach, A. R., and Taylor, R. **(1997)** Development and validation of a genetic algorithm for flexible docking. *J. Mol. Biol.* **267**, 727–748.

Jörnvall, H., Persson, B., Krook, M., Atrian, S., Gonzàlez-Duarte, R., Jeffery, J., and Ghosh, D. **(1995)** Short-Chain Dehydrogenases/reductases (SDR). *Biochemistry* **34**, 6003–6013.

Kallberg, Y., Oppermann, U., Jörnvall, H., and Persson, B. **(2002a)** Short-chain dehydrogenase/reductase (SDR) relationships: A large family with eight clusters common to human, animal, and plant genomes. *Protein Sci.* **11**, 636–641.

Kallberg, Y., Oppermann, U., Jörnvall, H., and Persson, B. **(2002b)** Short-chain dehydrogenases/reductases (SDRs). *Eur. J. Biochem.* **269**, 4409–4417.

Kallio, P., Sultana, A., Niemi, J., Mäntsälä, P., and Schneider, G. **(2006)** Crystal Structure of the Polyketide Cyclase AknH with Bound Substrate and Product Analogue: Implications for Catalytic Mechanism and Product Stereoselectivity. *J. Mol. Biol.* **357**, 210–220.

Kallio, P., Liu, Z., Mäntsälä, P., Niemi, J., and Metsä-Ketelä, M. **(2008a)** Sequential Action of Two Flavoenzymes, PgaE and PgaM, in Angucycline Biosynthesis: Chemoenzymatic Synthesis of Gaudimycin C. *Chemistry & Biology* **15**, 157–166.

Kallio, P., Liu, Z., Mäntsälä, P., Niemi, J., and Metsä-Ketelä, M. **(2008b)** A Nested Gene in Streptomyces Bacteria Encodes a Protein Involved in Quaternary Complex Formation. *J. Mol. Biol.* **375**, 1212–1221.

Kang, J.-H., McRoberts, J., Shi, F., Moreno, J. E., Jones, A. D., and Howe, G. A. **(2014)** The Flavonoid Biosynthetic Enzyme Chalcone Isomerase Modulates Terpenoid Production in Grandular Trichomes of Tomate. *Plant. Physiol.* **164**, 1161–1174.

Kavanagh, K. L., Jörnvall, H., Persson, B., and Oppermann, U. **(2008)** The SDR superfamily: functional and structural diversity within a family of metabolic and regulatory enzymes. *Cell. Mol. Life Sci.* **65**, 3895–3906.

Keatinge-Clay, A. T., and Stroud, R. M. **(2006)** The Structure of a Ketoreductase Determines the Organization of the β-Carbon Processing Enzymes of Modular Polyketide Synthases. *Structure* **14**, 737–748.

Keatinge-Clay, A. T. **(2007)** A Tylosin Ketoreductase Reveals How Chirality Is Determined in Polyketides. *Chem. Biol.* **14**, 898–908.

Kharel, M. K., Pahari, P., Shepherd, M. D., Tibrewal, N., Nybo, S. E., Shaaban, K. A., and and Rohr, J. **(2010)** Angucyclines: Biosynthesis, Mode-of-action, New Natural Products, and Synthesis. *Nat. Prod. Rep.* **29**, 264–325.

Kharel, M. K., Pahari, P., Shaaban, K. A., Wang, G., Morris, C., and Rohr, J. **(2012)** Elucidation of Post-PKS Tailoring Steps Involved in Landomycin Biosynthesis. *Org. Biomol. Chem.* **10**, 4256–4265.

Khersonsky, O., and Tawfik, D. S. **(2010)** Enzyme Promiscuity: A Mechanistic and Evolutionary Perspective. *Annu. Rev. Biochem.* **79**, 471–505.

Khosla, C., Tang, Y., Chen, A. Y., Schnarr, N. A., and Cane, D. E. **(2007)** Structure and Mechanism of the 6-Deoxyerythronolide B Synthase. *Annu. Rev. Biochem.* **76**, 195–221.

Khosla, C., Herschlag, D., Cane, D. E., and Walsh, C. T. **(2014)** Assembly Line Polyketide Synthases: Mechanistic Insights and Unsolved Problems. *Biochemistry* **53**, 2875–2883.

Korman, T. P., Hill, J. A., Vu, T. N., and Tsai, S. C. **(2004)** Structural Analysis of Actinorhodin Polyketide Ketoreductase: Cofactor Binding and Substrate Specificity. *Biochemistry* **43**, 14529−14538.

Korynevska, A., Heffeter, P., Matselyukh, B., Elbling, L., Micksche, M., Stoika, R., and Berger, W. **(2007)** Mechanisms underlying the anticancer activities of the angucycline landomycin E. *Biochem. Pharmocol.* **74**, 1713–1726.

Koskiniemi, H., Metsä-Ketelä, M., Dobrotzsch, D., Kallio, P., Korhonen, H., Mäntsälä, P., Schneider, G., and Niemi, J. **(2007)** Crystal Structures of Two Aromatic Hydroxylases Involved in the Early Tailoring Steps of Angucycline Biosynthesis. *J. Mol. Biol.* **372**, 633–648.

Lau, S. T. B., and Tanner, M. E. **(2008)** Mechanism and Active Site Residues of GDP-Fucose Synthase. *J. Am. Chem. Soc.* **130**, 17593–17602.

Link, S., Engelmann, K., Meierhoff, K., and Westhoff, P. **(2012)** The Atypical Short-Chain Dehydrogenases HCF173 and HCF244 Are Jointly Involved in Translational Initiation of the psbA mRNA of Arabidopsis. *Plant Physiol.* **160**, 2202–2218.

Lombo, F., Menendez, N., Salas, J. A., and Mendez, C. **(2006)** The aureolic acid family of antitumor compounds: structure, mode of action, biosynthesis, and novel derivatives. *Appl. Microbiol. Biotechnol.* **73**, 1–14.

Major, L. L., Wolucka, B. A., and Naismith, J. H. **(2005)** Structure and Function of GDP-Mannose-3',5'-Epimerase: An Enzyme which Performs Three Chemical Reactions at the Same Active Site. *J. Am. Chem. Soc.* **127**, 18309–18320.

Massey, V. **(2000)** The Chemical and Biological Versatility of Riboflavin. *Biochem. Soc. Trans.* **28**, 283–296.

Meksuriyen, D., and Cordell, G. A. **(1988)** Biosynthesis of Staurosporine, 2. Incorporation of Tryptophan. *J. Nat. Prod.* **51**, 893–899.

Metsä-Ketelä, M., Palmu, K., Kunnari, T., Ylihonko, T., and Mäntsälä, P. **(2003)** Engineering Anthracycline Biosynthesis Toward Angucyclines. *Antimicrob. Agents Chemother.* **47**, 1291–1296.

Metsä-Ketelä, M., Oja, T., Taguchi, T., Okamoto, S., and Ichinose, K. **(2013)** Biosynthesis of pyranonaphthoquinone polyketides reveals diverse strategies for enzymatic carbon-carbon bond formation. *Curr. Opin. Chem. Biol.* **17**, 562–570.

Minami, A., Shimaya, M., Suzuki, G., Migita, A., Shinde, S. S., Sato, K., Watanabe, K., Tamura, T., Oguri, H., and Oikawa, H. **(2012)** Sequential enzymatic Epoxidation Involved in Polyether Lasalocid Biosynthesis. *J. Am. Chem. Soc.* **134**, 7246–7249.

Moore, I. F., Hughes, D. W., and Wright, G. D. **(2005)** Tigecycline Is Modified by the Flavin-Dependent Monooxygenase TetX. *Biochemistry* **44**, 11829–11835.

Newman, D. J., and Cragg, G. M. **(2012)** Natural Products as Sources of New Drugs over the 30 Years from 1981 to 2010. *J. Nat. Prod.* **75**, 311–335.

Nguyen, H.-C., Darbon, E., Thai, R., Pernodet, J.-L., and Lautru, S. **(2013)** Post-PKS Tailoring Steps of the Spiramycin Macrolactone Ring in *Streptomyces ambofaciens*. *Antimicrob. Agents Chemother.* **57**, 3836–3842.

Niemi, J., Wang, Y., Aikas, K., Ylihonko, K., Hakala, J., and Mäntsälä, P. **(1999)** Characterization of aklavinone-11-hydroxylase from Streptomyces purpurascens. *Biochim. Biophys. Acta.* **1430**, 57–64.

O'Boyle, N. M., Tenderholt, A. L., and Langner, K. M. **(2008)** cclib: a Library for Package-Independent Computational Chemistry Algorithms. *J. Comput. Chem.* **29**, 839–845.

Oppermann, U., Filling, C., Hult, M., Shafqat, N., Wu, X., Lindh, M., Shafqat, J., Nordling, E., Kallberg, Y., Persson, B., and Jörnvall, H. **(2003)** Short-Chain Dehydrogenase/Reductases (SDR): the 2002 Update. *Chem.-Biol. Interact.* **143–144**, 247–253.

Osmanova, N., Schultze, W., and Ayoub, N. **(2010)** Azaphilones: a class of fungal metabolites with diverse biological activities. *Phytochem. Rev.* **9**, 315–342.

Palmu, K., Ishida, K., Mäntsälä, P., Hertweck, C., and Metsä-Ketelä, M. **(2007)** Artificial Reconstruction of Two Cryptic Angucycline Antibiotic Biosynthetic Pathways. *ChemBioChem* **8**, 1577–1584.

Palmu, K., and Kunnari, T. **(2002)** *PCT Int. Appl*, WO2002074800

Pahari, P., Kharel, M. K., Shepherd, M. D., van Lanen, S. G., and Rohr, J. **(2012)** Enzymatic Total Synthesis

of DefucogilvogarcinM and its Implications for Gilvogarcin Biosynthesis. *Angew. Chem. Int. Edit.* **51**, 1216−1220.

Pang, X., Aigle, B., Girardet, J.-M., Mangenot, S., Pernodet, J.-L., Decaris, B., and Leblond, P. **(2004)** Functional Angucycline-Like Antibiotic Gene Cluster in the Terminal Inverted Repeats of the *Streptomyces ambofaciens* Linear Chromosome. *Antimicrob. Agents Chemother.* **48**, 575–588.

Park, B. H., and Levy, S. B. **(1988)** The Cryptic Tetracycline Resistance Determinant on Tn4400 Mediates Tetracycline Degradation as Well as Tetracycline Efflux. *Antimicrob. Agents Chemother.* **32**, 1797–1800

Pearce, C. J., Doyle, T. W., Forenza, S., Lam, K. S., and Schroeder, R. **(1988)** The Biosynthesis of Rebeccamycin. *J. Nat. Prod.* **51**, 937–940.

Peric-Concha, N., Borovicka, B., Long, P. F., Hranueli, D., Waterman, P. G., and Hunter, I. S. **(2005)** Ablation of the *otcC* Gene Encoding a Post-polyketide Hydroxylase from the Oxytetracycline Biosynthetic Pathway in *Streptomyces rimosus* Results in Novel Polyketides with Altered Chain Length. *J. Biol. Chem.* **280**, 37455–37460.

Persson, B., Bray, J. E., Bruford, E., Dellaporta, S. L., Favia, A. D., Duarte, R. G., Jörnvall, H., Kallberg, Y., Kavanagh, K. L., Kedishvili, N.,Kisiela, M., Maser, E., Mindnich, R., Orchard, S., Penning, T. M., Thornton, J. M., Adamski, J, and Oppermann, U. **(2009)** The SDR (Short-Chain Dehydrogenase/Reductase and Related Enzymes) Nomenclature Initiative. *Chem. Biol. Interact.* **16**, 94–98.

Pickens, L. B., and Tang, Y. **(2010)** Oxytetracycline biosynthesis. *J. Biol. Chem.* **285**, 27509–27515.

Podschun B., Jahnke, K., Schnackerz, K. D., and Cook, P. F. **(1993)** Acid Base Catalytic Mechanism of the Dihydropyrimidine Dehydrogenase from pH Studies. *J. Biol. Chem.* **268**, 3407–3413.

Rix, U., Fischer, C., Remsing, L. L., and Rohr, J. **(2002)** Modification of post-PKS Tailoring Steps Through Combinatorial Biosynthesis. *Nat. Prod. Rep.* **19**, 542–580.

Rix, U., Remsing, L. L., Hoffmeister, D., Bechthold, A., and Rohr, J. **(2003)** Urdamycin L: a Novel Metabolic Shunt Product that Provides Evidence for the Role of the *urdM* gene in the Urdamycin A Biosynthetic Pathway of *Streptomyces fradiae* TÜ 2717. *ChemBioChem* **4**,109–111.

Rüegg, U. T., and Burgess, G. M. **(1989)** Staurosporine, K-252 and UCN-01: potent but nonspecific inhibitors of protein kinases. *Trends Pharmacol. Sci.* **10**, 218–220.

Rutkowski J., and Brzezinski, B. **(2013)** Structures and Properties of Naturally Occurring Polyether Antibiotics. *Biomed. Res. Int.* Article ID 162513.

Ryan, M. J. **(1999)** *U.S.Patent* 5,965,429.

Ryan, K. S., Howard-Jones, A. R., Hamill, M. J., Elliott, S. J., Walsh, C. T., and Drennan, C. L. **(2007)** Crystallographic Trapping in the Rebeccamycin Biosynthetic Enzyme RebC. *Proc. Natl. Acad. Sci. USA* **104**, 15311–15316.

Ryan, K. S., Chakraborty, S., Howard-Jones, A. R., Walsh, C. T., Ballou, D. P., and Drennan, C. L. **(2008)** The FAD Cofactor of RebC Shifts to an IN Conformation upon Flavin Reduction. *Biochemistry* **47**, 13506–13513.

Sanchez, C., Zhu, L., Brana, A. F., Salas, A. P., Rohr, J., Mendez, C., and Salas, J. A. **(2005)** Combinatorial biosynthesis of antitumor indolocarbazole compounds. *Proc. Natl. Acad. Sci. USA* **102**, 461–466.

Schuttelkopf, A. W., and van Alten, D. M. **(2004)** PRODRG: A Tool for High-Throughput Crystallography of Protein-Ligand complexes. *Acta Crystallogr. D* **60**, 1355–1363.

Shaaban, K. A., Stamatkin, C., Damodaran, C., and Rohr, J. **(2011)** 11-Deoxylandomycinone and Landomycins X-Z, New Cytotoxic Angucyclin(on)es from a *Streptomyces cyanogenus* K62 Mutant Strain. *J. Antibiot.* **64**, 141–150.

Sherman, D. H., Malpartida, F., Bibb, M. J., Kieser, H. M., Bibb, M. J., and Hopwood, D. A. **(1989)** Structure and deduced function of the granaticin-producing polyketide synthase gene cluster of *Streptomyces violaceoruber* Tü22. *EMBO J.* **8**, 2717–2725.

Shichijo, Y., Migita, A., Oguri, H., Watanabe, M., Tokiwano, T., Watanabe, K., and Oikawa, H. **(2008)** Epoxide Hydrolase Lsd19 for Polyether Formation in the Biosynthesis of Lasalocid A: Direct Experimental Evidence on Polyene-Polyepoxide Hypothesis in Polyether Biosynthesis. *J. Am. Chem. Soc.* **130**, 12230–12231.

Speer, B. S., and Salyers, A. A. **(1988)** Characterization of a Novel Tetracycline Resistance That Functions Only in Aerobically Grown *Escherichia coli*. *J. Bacteriol.* **170**, 1423–1429.

Stewart, C. Jr, Vickery, C. R., Burkart, M. D., and Noel, J. P. **(2013)** Confluence of Structural and Chemical Biology: Plant Polyketide Synthases as Biocatalysts for a Bio-Based Future. *Curr. Opin. Plant Biol.* **16**, 365–372.

Taguchi, T., Ebizuka, Y., Hopwood, D. A., and Ichinose, K. **(2001)** A New Mode of Stereochemical Control Revealed by Analysis of the Biosynthesis of

Dihydrogranaticin in *Streptomyces violaceoruber* Tü22. *J. Am. Chem. Soc.* **123**, 11376–11380.

Taguchi, T., Kunieda, K., Takeda-Shitaka, M., Takaya, D., Kawano, N., Kimberley, M. R., Booker-Milburn, K. I., Stephenson, G. R., Umeyama, H., Ebizuka, Y., and Ichinose, K. **(2004)** Remarkably Different Structures and Reaction Mechanisms of Ketoreductases for the Opposite Stereochemical Control in the Biosynthesis of BIQ Antibiotics. *Bioorg. Med. Chem.* **12**, 5917–5927.

Thibodeaux, C. J., Melançon, C. E. III, and Liu, H.-w. **(2008)** Natural-Product Sugar Biosynthesis and Enzymatic Glycodiversification. *Angew. Chem. Int. Ed.* **47**, 9814–9859.

Thoden, J. B., and Holden, H. M. **(1998)** Dramatic Differences in the Binding of UDP-Galactose and UDP-Glucose to UDP-Galactose 4-Epimerase from *Escherichia coli*. *Biochemistry* **37**, 11469–11477.

Trefzer, A., Salas, J. A., and Bechthold, A. **(1999)** Genes and enzymes involved in deoxysugar biosynthesis in bacteria. *Nat. Prod. Rep.* **16**, 283–299.

Trefzer, A., Fischer, C., Stockert, S., Westrich, L., Künzel, E., Girreser, U., Rohr, J., and Bechthold, A. **(2001)** Elucidation of the Function of Two Glycosyltransferase Genes (lanGT1 and lanGT4) Involved in Landomycin Biosynthesis and Generation of New Oligosaccharide Antibiotics. *Chem. Biol.* **8**, 1239–1252.

van Berkel, W. J. H., Kamerbeek, N. M., and Fraaije, M. W. **(2006)** Flavoprotein Monooxygenases, a diverse class of oxidative biocatalysts. *J. Biotechnol.* **124**, 670–689.

Vancurova, I., Volc, J., Flieger, M., Neuzil, J., Novotna, J., Vlach, J., and Behal, V. **(1988)** Isolation of Pure Anhydrotetracycline Oxygenase from *Streptomyces aureofaciens*. *Biochem. J.* **253**, 263–267.

Volkers, G., Palm, G. J., Weiss M. S., Wright G. D., and Hinrichs, W. **(2011)** Structural basis for a new tetracycline resistance mechanism relying on the TetX monooxygenase. *FEBS Letters* **585**, 1061–1066.

Volkers, G., Damas, J. M., Palm, G. J., Panjikar, S., Soares, C. M., and Hinrichs, W. **(2013)** Putative dioxygen-binding sites and recognition of tigecycline and minocycline in the tetracycline degrading monooxygenase TetX. *Acta Crystallogr. D* **69**, 1758–1767.

Walsh, C. T. **(2002)** Combinatorial Biosynthesis of Antibiotics: Challenges and Opportunities. *ChemBioChem* **3**, 124–134.

Wang, J., Ortiz-Maldonado, M., Entsch, B., Massey, V., Ballou, D., and Gatti, D. L. **(2002)** Protein and Ligand Dynamics in 4-Hydroxybenzoate Hydroxylase. *Proc. Natl. Acad. Sci. USA* **99**, 608–613.

Wang, P., Gao, X., and Tang, Y. **(2012a)** Complexity Generation During Natural Product Biosynthesis Using Redox Enzymes. *Curr. Opin. Chem. Biol.* **16**, 362–369.

Wang, P., Kim, W., Pickens, L. B., Gao, X., and Tang, Y. **(2012b)** Heterologous Expression and Manipulation of Three Tetracycline Biosynthetic Pathways. *Angew. Chem. Int. Ed.* **51**, 11136–11140.

Wang, P., Bashiri, G., Gao, X., Sawaya, M. R., and Tang, Y. **(2013)** Uncovering the Enzymes that Catalyze the Final Steps in Oxytetracycline Biosynthesis. *J. Am. Chem. Soc.* **135**, 7138–7141.

Westrich, L., Domann, S., Faust, B., Bedford, D., Hopwood, D.A., and Bechthold, A. **(1999)** Cloning and Characterization of a Gene Cluster from *Streptomyces cyanogenus* S136 Probably Involved in Landomycin Biosynthesis. *FEMS Microbiol. Lett.* **170**, 381–387.

Whicher, J. R., Dutta, S., Hansen, D. A., Hale, W. A., Chemler, J. A., Dosey, A. M., Narayan, A. R. H., Håkansson, K., Sherman, D. H., Smith, J. L., and Skiniotis, G. **(2014)** Structural rearrangements of a polyketide synthase module during its catalytic cycle. *Nature* **510**, 560–564.

Whittle, G., Hund, B. D., Shoemaker, N. B, and Salyers, A. A. **(2001)** Characterization of the 13-Kilobase *ermF* Region of the *Bacteroides* Conjugative Transposon CTnDOT. *Appl. Environ. Microbiol.* **67**, 3488–3495.

Wierenga, R. K., de Jong, R. J., Kalk, K. H., Hol, W. G., and Drenth, J. **(1979)** Crystal Structure of *p*-Hydroxybenzoate hydroxylase. *J. Mol. Biol.* **131**, 55–73.

Wright, G. D. **(2014)** Something Old, Something New: Revisiting Natural Products in Antibiotic Drug Discovery. *Can. J. Microbiol.* **60**, 147–154.

Yang, W., Moore, I. F., Koteva, K. P., Bareich, D. C., Hughes, D. W., and Wright, G. D. **(2004)** TetX Is a Flavin-Dependent Monooxygenase Conferring Resistance to Tetracycline Antibiotics. *J. Biol. Chem.* **279**, 52346–52352.

Zabala, A. O., Cacho, R. A., and Tang, Y. **(2012a)** Protein Engineering Towards Natural Product Synthesis and Diversification. *J. Ind. Microbiol. Biotechnol.* **39**, 227–241.

Zabala, A. O., Xu, W., Chooi, Y.-H., and Tang, Y. **(2012b)** Characterization of a Silent Azaphilone Gene Cluster from Aspergillus niger ATCC 1015 Reveals a Hydroxylation-Mediated Pyran-Ring Formation. *Chem. Biol.* **19**, 1049–1059.

Zhang, W., Watanabe, K., Cai, X., Jung, M. E., Tang, Y., and Zhan, J. **(2008)** Identifying the Minimal Enzymes Required for Anhydrotetracycline Biosynthesis. *J. Am. Chem. Soc.* **130**, 6068–6069.

Zheng, J., Taylor, C. A., Piasecki, S. K., and Keatinge-Clay, A. T. **(2010)** Structural and Functional Analysis of A-Type Ketoreductases from the Amphotericin Modular Polyketide Synthase. *Structure* **18**, 913–922.